isvr Institute of Sound and Vibration Research

# Investigation of the Radiation Efficiency of Strips

**G. Xie, D.J. Thompson and C.J.C. Jones**

ISVR Technical Memorandum No 895

October 2002

University of Southampton

# SCIENTIFIC PUBLICATIONS BY THE ISVR

***Technical Reports*** are published to promote timely dissemination of research results by ISVR personnel. This medium permits more detailed presentation than is usually acceptable for scientific journals. Responsibility for both the content and any opinions expressed rests entirely with the author(s).

***Technical Memoranda*** are produced to enable the early or preliminary release of information by ISVR personnel where such release is deemed to the appropriate. Information contained in these memoranda may be incomplete, or form part of a continuing programme; this should be borne in mind when using or quoting from these documents.

***Contract Reports*** are produced to record the results of scientific work carried out for sponsors, under contract. The ISVR treats these reports as confidential to sponsors and does not make them available for general circulation. Individual sponsors may, however, authorize subsequent release of the material.

UNIVERSITY OF SOUTHAMPTON

INSTITUTE OF SOUND AND VIBRATION RESEARCH

DYNAMICS GROUP

# Investigation of the Radiation Efficiency of Strips

by

**G. Xie, D.J. Thompson and C.J.C. Jones**

ISVR Technical Memorandum No: 895

October 2002

Authorised for issue by
Dr M.J. Brennan
Group Chairman

# ABSTRACT

The average radiation efficiency of rectangular plates is investigated by using the modal summation based on the far-field sound intensity. It is found that the total radiation can be predicted using a sum of modal contributions without the need to include cross terms, provided that a 'rain on the roof' excitation is considered. The numerical results from the modal summation are compared with formulae from previous literature. In the acoustic-circulating region the published formulae are not applicable for predicting the average radiation efficiency for a strip, a plate with a very large aspect ratio. Further analysis for the strip reveals that the radiation efficiency at frequencies below the fundamental frequency is proportional to the square of the shortest edge length. An approximation for calculating the average radiation efficiency of the strip is derived. The effect of damping on the average radiation efficiency is also investigated by numerical results and found to have quite a large effect between the first and second cut-on frequencies of the strip. The maximum radiation efficiency around the critical frequency is found to vary less with *ka* than published models suggest. Finally an analytical method for the radiation efficiency of a double-walled extruded plate is given in terms of global and local modes, where the analysis combines the results from both rectangular plates and strips.

# CONTENTS

# 1 INTRODUCTION

The subject of sound radiation from vibrating structures is of great practical importance. Many structures of practical interest may be modelled sufficiently accurately by rectangular, uniform flat plates. Although they are generally dynamically coupled in real systems to contiguous structures, the isolated rectangular panel is useful to illustrate the radiation from bending waves. This subject has been investigated extensively over the last few decades.

For a flat plate set in an infinite baffle, there are two common approaches to determine the radiation efficiency or resistance theoretically. The first is to integrate the far-field acoustic intensity over a hemisphere enclosing the plate. The other approach is to integrate the acoustic intensity over the surface of the vibrating plate. Both approaches require the knowledge of the distribution of vibration velocity over the plate, which is usually obtained by assuming the boundary conditions are simple supports. Since plate vibrations generally involve many superposed modes, the radiation efficiency of a plate, in principle, can be obtained by summing the effect of all the modes that contribute significantly in the frequency range under consideration. The radiation efficiency of a single mode of the plate is usually called the modal radiation efficiency. The total radiation efficiency of the plate is called either the average radiation efficiency or the weighted radiation efficiency. In the literature both the radiation resistance and the radiation efficiency are used, the latter being the radiation resistance normalised by the surface area and the impedance of air. The radiation efficiency is defined by

$$\sigma = \frac{R_{rad}}{\rho c S} = \frac{W_{rad}}{\rho c S \left\langle \overline{u^2} \right\rangle} \tag{1.1}$$

where $R_{rad}$ is radiation resistance, $W_{rad}$ is power radiated by the plate, $S$ is the area of the plate, $\left\langle \overline{u^2} \right\rangle$ is the spatial mean square velocity of the plate vibration, $\rho$ and $c$ are the density of air and the speed of sound in air.

As early as the 1960s, Maidanik [1] first proposed several approximate formulae for calculating the modal radiation resistance in the whole frequency range. Wallace [2] presented exact and approximate expressions for the modal radiation efficiency of rectangular plates at arbitrary frequencies below the critical frequency. He investigated the effects on radiation efficiency of the inter-nodal areas and their aspect ratios. The characteristics of the radiation from a baffled

rectangular plate were clearly shown. Gomperts [3, 4] investigated the modal radiation of a rectangular plate under general boundary conditions. It was found by Gomperts that plates with greater edge-constraints do not always have larger radiation efficiencies than less edge-constrained ones, and the radiation efficiencies for two-dimensional vibration patterns differ rather considerably from those for one-dimensional vibration patterns. Heckl [5] analysed sound radiation of planar sources by using a Fourier transform approach in $k$-space (wavenumber space). Leppington [6] later introduced several asymptotic formulae to calculate the modal radiation efficiency for large acoustic wavenumbers, especially in the range close to the critical frequency. Williams [7] proposed a series expansion in ascending powers of the wavenumber $k$ for the acoustic power radiated from a planar source. Most recently, Li [8] gave an analytical solution, in the form of a power series of the non-dimensional acoustic wavenumber, to calculate the modal radiation resistance of a rectangular plate for moderate wavenumbers.

The average radiation of a plate has also been an active subject of study because of its practical importance. It was also Maidanik [1] who first applied the concept of power flow and statistical energy analysis to overcome the burdensome calculation at higher frequencies where many modes are contributing. He presented a formula for the average radiation resistance based on the assumption of a reverberant vibration field (equal modal energy). A similar modal-average radiation curve was presented in reference [9]. Leppington [6] re-investigated the problem of average radiation efficiency and gave some revision of Maidanik's work by using the assumption of high modal densities for the plate. His assumption is based on same principle as Maidanik's. It was found in Leppington's study that Maidanik overestimates the radiation resistance at coincidence, particularly for a plate with very large aspect ratio. However, in the works of both Maidanik and Leppington, the radiation resistance was considered without including the cross-mode contributions. Snyder and Tanaka [10] introduced the contribution of the cross-modal couplings to calculate the total acoustic power at low frequency using modal radiation efficiencies. It was shown that the cross-mode contributions are only non-zero for pairs of modes that are both either odd or even in a given direction. The mutual radiation resistance was also investigated recently by Li and Gibeling [11, 12]. It was found that the cross-modal coupling could have a significant impact on the radiated power, even at a resonance frequency. The cross-modal contributions were also included in the power series of Li [8].

Currently, an investigation is underway into the acoustic and dynamic characteristics of double-walled extruded plates as used in railway vehicles [13]. As part of this work, it is required to model the sound radiation and transmission of such extruded plates. The extruded plate can be

considered as a built-up structure composed of a set of strips with their long edges having same length and the short edges having different lengths. The natural modes of the extruded plate can be separated into the global modes of the whole plate, particularly at low frequency, and the local modes of the various strips at high frequency [13]. The local modes are dominated by the dynamic behaviour of a single strip. The consideration of the sound radiation of the strip essentially involves the sound radiation of a rectangular plate. However, it will be shown that, for frequencies well below the critical frequency, the classic formulae previously obtained from the rectangular plate are not suitable for the strip, which has a large aspect ratio. Sakagami [14] investigated the characteristic of the sound field radiated by the strip under different excitation. But only the sound pressure for certain given position was studied. The radiation efficiency of the strip is still less investigated.

The present report is carried out to investigate this problem. The average radiation efficiency of a rectangular plate is considered first in terms of the summation of the normal modes. The average radiation efficiency of a strip is then investigated. An approximate formula applicable at frequencies below the critical frequency is developed and compared with the results from a numerical integration. Finally an analytical method for the radiation efficiency of a double-walled extruded plate is given.

# 2 MODAL RADIATION EFFICIENCY

The modal radiation efficiency of a rectangular plate can be obtained by the integral of the far-field acoustic intensity [2]. It can also be obtained by integration of the intensity over the plate surface but this is less usual in the literature. The plate is assumed to vibrate in one of its natural frequencies with simple supports and to be set in an infinite baffle. It is well known that, below the critical frequency, the odd-odd modes give higher radiation efficiency than odd-even and even-even modes because the latter suffer more cancellation of radiation [2]. Above the critical frequency, the radiation efficiency approaches unity, provided that the plate is also large compared to the acoustic wavelength. For plates with different aspect ratios, these conclusions are always valid.

Before the radiation of the strip is considered, it should be indicated that the boundary conditions of the strip edges are supposed here to be simple supports as in [2]. There are two reasons for

this choice. Based on the investigation of the mode count of the extruded plate by the present authors [13], the boundary conditions between strips were found to be between simple supports and clamped. The two short edges of the strips could be considered as simple supports and the other two as between simple supports and clamped. However, Gomperts [4] showed that the radiation efficiency of such a hinged-clamped plate is almost equal to that of the hinged-hinged (simply supported) plate. Therefore it is reasonable to assume that the strips of an extruded plate are simply supported for the purpose of calculating the sound radiation of the strips. Secondly, as the modes of such a plate are simple sine functions this considerably simplifies calculations.

The plate is assumed to be flat and lie in an infinite baffle in order that the Rayleigh integral technique may be used.

Considering a simply supported strip in an infinite baffle, the expression for the modal radiation obtained by integrating the far-field acoustic intensity is given by Wallace [2] as

$$\sigma_{mn} = \frac{64k^2ab}{\pi^6 m^2 n^2} \int_0^{\pi/2} \int_0^{\pi/2} \left\{ \frac{\cos\left(\frac{\alpha}{2}\right)\cos\left(\frac{\beta}{2}\right)}{\sin\left(\frac{\alpha}{2}\right)\sin\left(\frac{\beta}{2}\right)} \right\}^2 \left[ \left( \frac{\alpha}{m\pi} \right)^2 - 1 \right] \left[ \left( \frac{\beta}{n\pi} \right)^2 - 1 \right] \sin\theta d\theta d\phi \qquad (2.1)$$

where $a$ and $b$ are the dimensions of the plate, $m$ and $n$ are the indices of modes (number of half sine waves across the length and width directions), $k$ is the acoustic wavenumber, and $\alpha = ka\sin\theta\cos\phi$ and $\beta = kb\sin\theta\cos\phi$. The cosine terms apply when $m$ or $n$ odd and sine terms when $m$ or $n$ are even.

Approximate expressions for the modal radiation efficiency at arbitrary frequencies below the critical frequency were also given by Wallace [2] as

$$\sigma_{mn} \simeq \frac{32(ka)(kb)}{m^2 n^2 \pi^5} \left\{ 1 - \frac{k^2 ab}{12} \left[ \left( 1 - \frac{8}{(m\pi)^2} \right) \frac{a}{b} + \left( 1 - \frac{8}{(n\pi)^2} \right) \frac{b}{a} \right] \right\} \quad m,n \text{ odd} \qquad (2.2)$$

$$\sigma_{mn} \simeq \frac{8(ka)(kb)^3}{3m^2 n^2 \pi^5} \left\{ 1 - \frac{k^2 ab}{20} \left[ \left( 1 - \frac{8}{(m\pi)^2} \right) \frac{a}{b} + \left( 1 - \frac{24}{(n\pi)^2} \right) \frac{b}{a} \right] \right\} \quad m \text{ odd}, n \text{ even} \qquad (2.3)$$

$$\sigma_{mn} \simeq \frac{2(ka)^3(kb)^3}{15m^2 n^2 \pi^5} \left\{ 1 - \frac{5k^2 ab}{64} \left[ \left( 1 - \frac{24}{(m\pi)^2} \right) \frac{a}{b} + \left( 1 - \frac{24}{(n\pi)^2} \right) \frac{b}{a} \right] \right\} \quad m,n \text{ even} \qquad (2.4)$$

From the power of $k$ in these expressions, it can be seen that odd-odd modes are most effective in radiation and even-even modes are least effective.

Figure 2.1 presents the radiation efficiency calculated using equation (2.1) of the first few modes of an aluminium strip of dimension 0.16×3m. The thickness of the strip is arbitrary. It can be seen that the odd-odd modes have the highest radiation efficiency. Moreever, the lowest order modes have the highest radiation efficiency at low frequency. In each case the radiation efficiency reaches unity at high frequencies.

Note that some results at high frequencies become unreliable due to the integration of a strongly oscillating function.

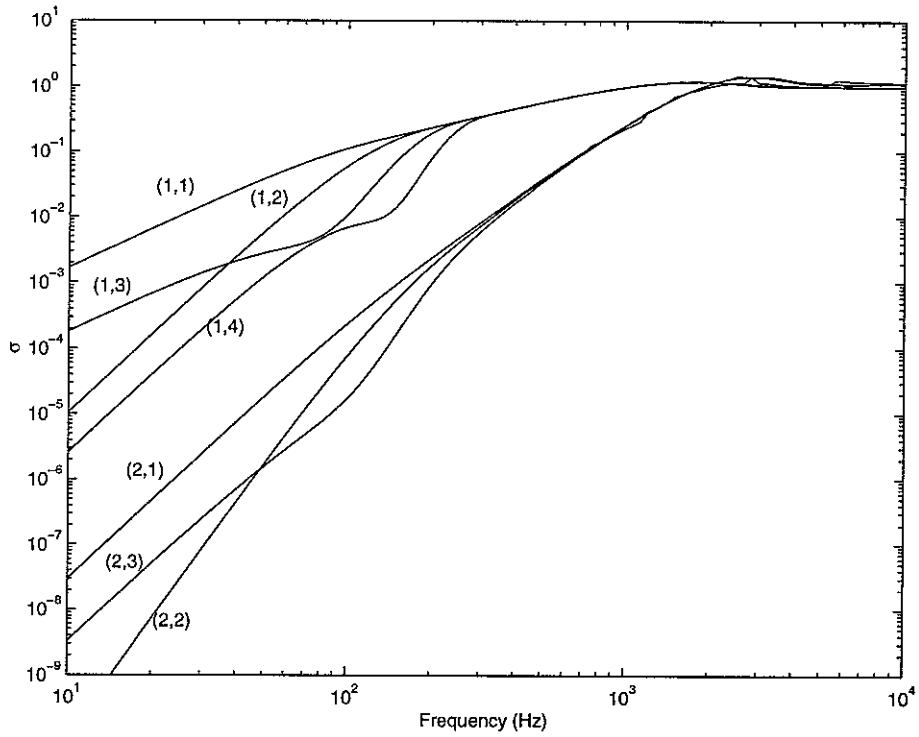


**Figure 2.1 Modal radiation efficiency of a strip 0.16×3m.**

# 3 AVERAGE RADIATION EFFICIENCY

In actual engineering applications, the modal radiation efficiency is not really useful because the plate vibrations generally involve many superposed modes. The average radiation efficiency is of greater importance. In principle, the average radiation efficiency of a plate can be determined if the velocity at every point on the plate is known as a function of frequency. It is also possible to

evaluate the average radiation efficiency from the velocity amplitudes and the radiation efficiency of all participating modes. Since the amplitude of each mode depends not only on the ratio of the excitation frequency to the resonance frequency of the mode, but also on the spatial distribution of the excitation, it is almost impossible to know the total radiation efficiency in practice. However, if the uncertainties are accepted to some extent, a statistical result can be obtained from general considerations, such as the use of a rain on the roof excitation, and this can be useful in practice. Such an approach is considered here.

## 3.1 AVERAGE RADIATION EFFICIENCY

### 3.1.1 SOUND POWER IN TERMS OF PLATE MODES

Consider a rectangular plate, simply supported on four edges and set in an infinite rigid baffle as shown in Figure 3.1.

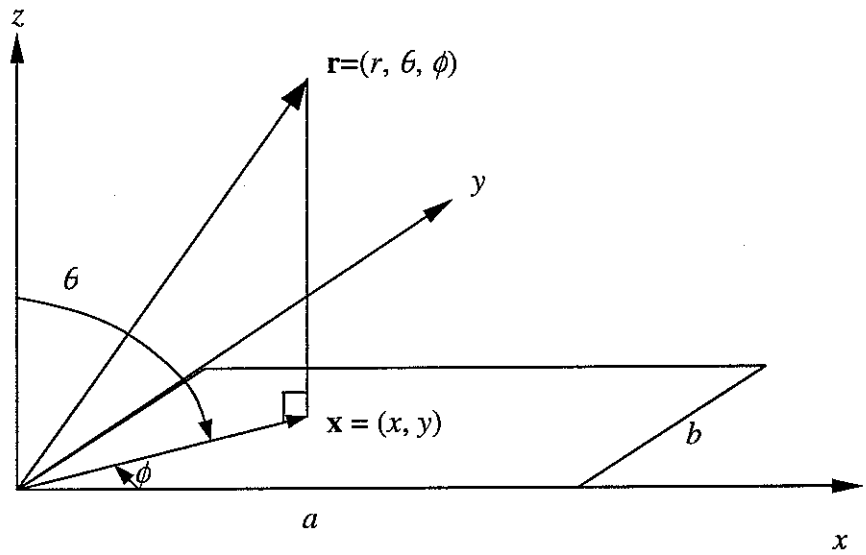


**Figure 3.1 Coordinate system of a vibrating rectangular plate.**

The total acoustic power radiated from the plate can be obtained by integrating the far-field acoustic intensity to give

$$W = \int_0^{2\pi} \int_0^{\pi/2} \frac{|p(\mathbf{r})|^2}{2\rho c} r^2 d\theta d\phi \tag{3.1}$$

where $p(\mathbf{r})$ is the complex acoustic pressure amplitude at a location in space expressed in spherical coordinates, $\mathbf{r} = (r, \theta, \phi)$ at frequency $\omega$.

The complex acoustic pressure $p(\mathbf{r})$ can be written in terms of the plate surface velocity using the Rayleigh integral [15],

$$p(\mathbf{r}) = \frac{jk\rho c}{2\pi}\int_s u(\mathbf{x})\frac{e^{-jkr}}{r}d\mathbf{x} \tag{3.2}$$

where $u(\mathbf{x})$ is the complex surface velocity amplitude at location $\mathbf{x} = (x, y)$, $k$ is the acoustic wavenumber and the integral is evaluated over the plate surface. The distance $r = |\mathbf{r} - \mathbf{x}|$.

The velocity $u(\mathbf{x})$ at any location $\mathbf{x}$ on the structure can be found by superposing the modal contributions as

$$u(\mathbf{x}) = \sum_{m=1}^{\infty}\sum_{n=1}^{\infty} u_{mn}\varphi_{mn}(\mathbf{x}) \tag{3.3}$$

where $u_{mn}$ is the complex velocity amplitude of the mode $(m, n)$, $\varphi_{mn}(\mathbf{x})$ is the value of the associated mode shape function at the location $\mathbf{x}$, and $m$, $n$ are the indices of the modes. $u_{mn}$ depends on the form of the excitation and on frequency. The mode shape function $\varphi_{mn}(\mathbf{x})$ for the simply supported rectangular plate can be expressed as

$$\varphi_{mn}(x, y) = \sin\left(\frac{m\pi x}{a}\right)\sin\left(\frac{n\pi y}{b}\right) \tag{3.4}$$

Substituting equation (3.3) and (3.4) into (3.2), the sound pressure is given by

$$p(\mathbf{r}) = \frac{jk\rho c}{2\pi}\int_s \sum_{m=1}^{\infty}\sum_{n=1}^{\infty} u_{mn}\varphi_{mn}(\mathbf{x})\frac{e^{-jkr}}{r}d\mathbf{x}$$

$$p(\mathbf{r}) = \sum_{m=1}^{\infty}\sum_{n=1}^{\infty} u_{mn}\left\{\frac{jk\rho c}{2\pi}\int_s \varphi_{mn}(\mathbf{x})\frac{e^{-jkr}}{r}d\mathbf{x}\right\} \tag{3.5}$$

From Wallace [2], the integral in the brackets, called $A_{mn}(\mathbf{r})$ here, is given by

$$A_{mn}(\mathbf{r}) = jk\rho c\frac{e^{-jkr}}{2\pi r}\frac{ab}{\pi^2 mn}\left[\frac{(-1)^m e^{j\alpha} - 1}{\left(\frac{\alpha}{m\pi}\right)^2 - 1}\right]\left[\frac{(-1)^n e^{j\beta} - 1}{\left(\frac{\beta}{n\pi}\right)^2 - 1}\right] \tag{3.6}$$

where $\alpha = ka\sin\theta\cos\phi$ and $\beta = kb\sin\theta\sin\phi$, and $r$ is now $|\mathbf{r}|$.

The sound pressure $p(\mathbf{r})$ is now expressed as

$$p(\mathbf{r}) = \sum_{m=1}^{\infty}\sum_{n=1}^{\infty} u_{mn}A_{mn}(\mathbf{r}) \tag{3.7}$$

The substitution of equation (3.7) into equation (3.1) gives the total radiated power of the plate as

$$W = \int_0^{2\pi}\int_0^{\pi/2} \frac{p(\mathbf{r})p^*(\mathbf{r})}{2\rho c} r^2 d\theta d\phi$$

$$W = \int_0^{2\pi}\int_0^{\pi/2} \frac{\sum_{m=1}^{\infty}\sum_{n=1}^{\infty} u_{mn}A_{mn}(\mathbf{r}) \sum_{m'=1}^{\infty}\sum_{n'=1}^{\infty} u^*_{m'n'}A^*_{m'n'}(\mathbf{r})}{2\rho c} r^2 d\theta d\phi$$

$$W = \sum_{m=1}^{\infty}\sum_{n=1}^{\infty}\sum_{m'=1}^{\infty}\sum_{n'=1}^{\infty}\left\{ u_{mn}u^*_{m'n'} \int_0^{2\pi}\int_0^{\pi/2} \frac{A_{mn}(\mathbf{r})A^*_{m'n'}(\mathbf{r})}{2\rho c} r^2 d\theta d\phi \right\} \tag{3.8}$$

where $p^*(\mathbf{r})$ is the conjugate of the sound pressure $p(\mathbf{r})$, and $m'$ and $n'$ are used to distinguish $m$ and $n$ in the conjugate. From this equation, it can be seen that the total radiated power depends on the contribution of combinations of modes. The contribution is usually referred as self-modal radiation for $m = m'$ and $n = n'$, and cross-modal radiation otherwise for either $m \neq m'$ or $n \neq n'$.

The equation (3.8) can also be expressed in a matrix form,

$$W = \mathbf{u}^{\mathrm{T}}\mathbf{A}\mathbf{A}^{\mathrm{T}}\mathbf{u} \tag{3.9}$$

in which the diagonal elements of $\mathbf{A}\mathbf{A}^{\mathrm{T}}$ are self-modal terms and the off-diagonal elements are mutual radiation terms. According to Snyder and Tanaka [10], the cross-modal radiation only occurs between a pair of modes with a similar index-type (ie even or odd in both directions). Hence, only a quarter of the off-diagonal elements are non-zero.

It is clear that the calculation of total radiation efficiency requires the calculation of both self- and cross-modal radiation terms described in equation (3.8). At same time, the knowledge of the excitation is also required to give $\mathbf{u}$.

### 3.1.2 RESPONSE TO POINT FORCE

Consider a point force applied on the plate at location $(x_0, y_0)$. The modal velocity amplitude is given by [16]

$$u_{mn} = \frac{j\omega P\varphi_{mn}(x_0, y_0)}{\left[\omega_{mn}^2(1+j\eta) - \omega^2\right]M_{mn}} \tag{3.10}$$

where $P$ is the force amplitude, $\omega_{mn}$ is the natural frequency, $\eta$ is the damping loss factor assuming hysteretic damping and $M_{mn}$ is the modal mass that is given by

$$M_{mn} = \int_S \rho_s h \varphi_{mn}^2 (x,y) dS = \frac{1}{4} \rho_s hab = \frac{M}{4} \tag{3.11}$$

where $\rho_s$ and $h$ are the density and thickness of the plate $M$ is the mass the plate and use is made of the form of $\varphi_{mn}$ from equation (3.4).

The natural frequencies $\omega_{mn}$ are given by

$$\omega_{mn} = \left( \frac{B}{\rho_s h} \right)^{\frac{1}{2}} \left[ \left( \frac{m\pi}{a} \right)^2 + \left( \frac{n\pi}{b} \right)^2 \right] \tag{3.12}$$

where $B$ is the bending stiffness of the plate.

For the purpose of obtaining a general guideline for the total radiated power, consider the average of all possible locations of the uncorrelated point forces on the plate. This average total radiated power can be written as

$$\overline{W} = \frac{1}{ab} \int_0^a \int_0^b W dx_0 dy_0 \tag{3.13}$$

$$\overline{W} = \sum_{m=1}^{\infty} \sum_{n=1}^{\infty} \sum_{m'=1}^{\infty} \sum_{n'=1}^{\infty} \left\{ \frac{1}{ab} \int_0^a \int_0^b u_{mn} u_{m'n'}^* dx_0 dy_0 \int_0^{2\pi} \int_0^{\pi/2} \frac{A_{mn}(\mathbf{r}) A_{m'n'}^*(\mathbf{r})}{2\rho c} r^2 d\theta d\phi \right\} \tag{3.14}$$

where

$$\int_0^a \int_0^b u_{mn} u_{m'n'}^* dx_0 dy_0 = \int_0^a \int_0^b \left[ \frac{j\omega P \varphi_{mn}(x_0, y_0)}{\left[ \omega_{mn}^2 (1 + j\eta) - \omega^2 \right] M_{mn}} \frac{-j\omega P \varphi_{m'n'}(x_0, y_0)}{\left[ \omega_{m'n'}^2 (1 - j\eta) - \omega^2 \right] M_{m'n'}} \right] dx_0 dy_0$$

Because of the orthogonality of the eigenfunctions,

$$\int_0^a \int_0^b \varphi_{mn}(x_0, y_0) \varphi_{m'n'}(x_0, y_0) dx_0 dy_0 = 0 \quad \text{for } m \neq m' \text{ or } n \neq n' \tag{3.15}$$

and equation (3.14) can be simplified as

$$\overline{W} = \sum_{m=1}^{\infty} \sum_{n=1}^{\infty} \left\{ \frac{1}{ab} \int_0^a \int_0^b u_{mn} u_{mn}^* dx_0 dy_0 \int_0^{2\pi} \int_0^{\pi/2} \frac{A_{mn}(\mathbf{r}) A_{mn}^*(\mathbf{r})}{2\rho c} r^2 d\theta d\phi \right\} \tag{3.16}$$

where each term in the sum is the power radiated by a single mode. Equation (3.16) can also be written as

$$\overline{W} = \sum_{m=1}^{\infty} \sum_{n=1}^{\infty} \overline{W}_{mn} \tag{3.17}$$

where $\overline{W}_{mn}$ can be expressed as

$$\overline{W}_{mn} = \overline{|u_{mn}|^2} \int_0^{2\pi} \int_0^{\pi/2} \frac{A_{mn}(\mathbf{r}) A^*_{m'n'}(\mathbf{r})}{2\rho c} r^2 d\theta d\phi \tag{3.18}$$

where $\overline{|u_{mn}|^2}$ represents the modulus squared of the modal velocity amplitude $u_{mn}$, averaged over all force positions.

The power radiated by the mode ($m$, $n$) can also given in terms of its radiation efficiency by

$$\overline{W}_{mn} = \sigma_{mn} \rho c a b \overline{\langle u_{mn}^2 \rangle} \tag{3.19}$$

where $\overline{\langle u_{mn}^2 \rangle}$ represents the spatially-averaged mean square velocity in mode ($m$, $n$) averaged over all possible force positions.

The average modulus squared of the velocity amplitude $\overline{|u_{mn}|^2}$ is given by

$$\begin{aligned}
\overline{|u_{mn}|^2} &= \frac{1}{ab} \int_0^a \int_0^b u_{mn} u^*_{mn} dx_0 dy_0 \\
&= \frac{1}{ab} \int_0^a \int_0^b \frac{\omega^2 P^2 \varphi_{mn}^2(x_0, y_0)}{\left[ \left( \omega_{mn}^2 - \omega^2 \right)^2 + \eta^2 \omega_{mn}^4 \right] M_{mn}^2} dx_0 dy_0 \\
&= \frac{\omega^2 P^2}{ab \rho_p h \left[ \left( \omega_{mn}^2 - \omega^2 \right)^2 + \eta^2 \omega_{mn}^4 \right] M_{mn}} \\
&= \frac{4\omega^2 P^2}{M^2 \left[ \left( \omega_{mn}^2 - \omega^2 \right)^2 + \eta^2 \omega_{mn}^4 \right]}
\end{aligned} \tag{3.20}$$

The spatially-averaged mean square velocity amplitude in mode ($m$, $n$) due to a point force at ($x_0$, $y_0$) is defined by

$$\overline{\langle u_{mn}^2 \rangle} = \frac{1}{S} \int_S \left[ \frac{1}{T} \int_0^T \left| u_{mn}(x, y, t) \right|^2 \right] dS, \tag{3.21}$$

where $T$ is a period of time over which to estimate the mean square velocity at any position on the plate, and $S$ is the area of the plate. For the present case,

$$\begin{aligned}\overline{\left\langle u_{mn}^2 \right\rangle} &= \frac{1}{S}\int_S \left[\frac{1}{2}\left|u_{mn}(x,y)\right|^2\right] dxdy \\ &= \frac{1}{2S}\left|u_{mn}\right|^2 \int_S \varphi_{mn}^2(x,y)dxdy \\ &= \frac{1}{8}\left|u_{mn}\right|^2 \\ &= \frac{1}{8}\frac{\omega^2 P^2 \varphi_{mn}^2(x_0,y_0)}{\left[\left(\omega_{mn}^2-\omega^2\right)^2+\eta^2\omega_{mn}^4\right]M_{mn}^2}\end{aligned} \tag{3.22}$$

If the average is taken over all possible force locations, this average spatially-averaged mean square velocity is given by

$$\begin{aligned}\overline{\left\langle u_{mn}^2 \right\rangle} &= \frac{1}{S}\int_S \left\langle \overline{u_{mn}^2} \right\rangle dx_0 dy_0 \\ &= \frac{1}{S}\int_S \frac{1}{8}\frac{\omega^2 P^2 \varphi_{mn}^2(x_0,y_0)}{\left[\left(\omega_{mn}^2-\omega^2\right)^2+\eta^2\omega_{mn}^4\right]M_{mn}^2} dx_0 dy_0 \\ &= \frac{1}{8M}\frac{\omega^2 P^2}{\left[\left(\omega_{mn}^2-\omega^2\right)^2+\eta^2\omega_{mn}^4\right]M_{mn}} \\ &= \frac{1}{2M^2}\frac{\omega^2 P^2}{\left[\left(\omega_{mn}^2-\omega^2\right)^2+\eta^2\omega_{mn}^4\right]}\end{aligned} \tag{3.23}$$

From equations (3.20) and (3.23), it can be seen that

$$\overline{\left|u_{mn}\right|^2} = 8\overline{\left\langle u_{mn}^2 \right\rangle} \tag{3.24}$$

Having obtained the total radiated power in terms of a summation of modal radiated power, the average radiation efficiency considering all possible point force locations is readily given from equation (1.1) by

$$\sigma = \frac{\sum_{m=1}^{\infty}\sum_{n=1}^{\infty}\overline{W}_{mn}}{\rho cab\overline{\left\langle u^2 \right\rangle}} = \frac{\sum_{m=1}^{\infty}\sum_{n=1}^{\infty}\rho cab\sigma_{mn}\overline{\left\langle u_{mn}^2 \right\rangle}}{\rho cab\overline{\left\langle u^2 \right\rangle}} = \frac{\sum_{m=1}^{\infty}\sum_{n=1}^{\infty}\sigma_{mn}\overline{\left\langle u_{mn}^2 \right\rangle}}{\overline{\left\langle u^2 \right\rangle}} \tag{3.25}$$

where $\overline{\left\langle u^2 \right\rangle}$ is the average spatial mean square velocity if all possible force locations are considered. This spatial mean square velocity is given by [16]

$$\overline{\left\langle u^2 \right\rangle} = \frac{\omega^2 P^2}{2M^2}\sum_{m=1}^{\infty}\sum_{n=1}^{\infty}\frac{1}{\left[\left(\omega_{mn}^2-\omega^2\right)^2+\eta^2\omega_{mn}^4\right]} = \sum_{m=1}^{\infty}\sum_{n=1}^{\infty}\overline{\left\langle u_{mn}^2 \right\rangle} \tag{3.26}$$

Hence,

$$\sigma = \frac{\sum_{m=1}^{\infty}\sum_{n=1}^{\infty}\sigma_{mn}\left[\left(\omega_{mn}^2-\omega^2\right)^2+\eta^2\omega_{mn}^4\right]^{-1}}{\sum_{m=1}^{\infty}\sum_{n=1}^{\infty}\left[\left(\omega_{mn}^2-\omega^2\right)^2+\eta^2\omega_{mn}^4\right]^{-1}} \tag{3.27}$$

It is noted that this average radiation efficiency depends only on the self-modal radiations due to the averaging over all possible force locations. Equation (3.25) corresponds with that from Cremer and Heckl [16], who analysed the radiation power using a wavenumber transform.

### 3.1.3 PREVIOUS RESULTS

Based on the assumption of a diffuse field in the plate, Maidanik (1962) and Leppington (1982) have produced expressions for the modal-average radiation without including cross-modal radiation. The expression of Maidanik [1] is given by

$$\sigma = \begin{cases} \dfrac{4S}{c^2}f^2 & \text{for } f < f_{1,1} \\ \dfrac{4\pi^2}{c^2 S}\dfrac{D}{m''} & \text{for } f_{1,1} < f < f_e, \quad f_e = \dfrac{3c}{P} \\ \dfrac{Pc}{4\pi^2 S f_c}\times\dfrac{\left(1-\alpha^2\right)\ln\left(\dfrac{1+\alpha}{1-\alpha}\right)+2\alpha}{\left(1-\alpha^2\right)^{3/2}} & \text{for } f_e < f < f_c, \quad \alpha = \sqrt{\dfrac{f}{f_c}} \\ 0.45\sqrt{\dfrac{Pf_c}{c}} & \text{for } f = f_c \\ \left(1-\dfrac{f_c}{f}\right)^{-1/2} & \text{for } f > f_c \end{cases} \tag{3.28}$$

where $c$ is speed of sound, $f$ is frequency, $P$ is now the perimeter of the plate, $S$ is the area of the plate, $f_c$ is the critical frequency, $D$ is the bending stiffness and $m''$ is the mass per unit area of the plate. NB an additional term in the third expression is presented in [1] but is often omitted.

The expression of Leppington [6] is given by

$$\sigma = \begin{cases} \dfrac{P}{2\pi\mu k S\left(\mu^2-1\right)^{\frac{1}{2}}}\left[\ln\left(\dfrac{1+\mu}{1-\mu}\right)+\dfrac{2\mu}{\mu^2-1}\right] & \mu>1, ka_1(\mu-1) \text{ large;} \\ k^{\frac{1}{2}}a_1^{\frac{1}{2}}H(\gamma) & \mu=1; \\ \left(1-\mu^2\right)^{-\frac{1}{2}} & \mu<1, ka_1(1-\mu) \text{ large;} \end{cases} \tag{3.29}$$

where $a_1$, $a_2$ are the lesser and the greater of $a$ and $b$, $k$ is the acoustic wavenumber, $\gamma$is the $a_1/a_2$ and $\mu$ is the ratio of the structure wavenumber to the acoustic wavenumber. The function $H(\gamma)$ is defined by

$$H(x)=\frac{4}{15\pi^{\frac{3}{2}}}x^{\frac{1}{2}}\int_0^1(5-t)\left\{\left(t^2+x^2\right)^{-\frac{3}{4}}+\left(1+x^2t^2\right)^{-\frac{3}{4}}\right\}dt, \tag{3.30}$$

For $0.2 < x < 1$, a good approximation of $H(x)$ is given by $H(x)=0.5-0.15x$.

### 3.1.4 RESULTS

A MATLAB program has been produced to evaluate equation (3.25). The modal radiation efficiency is calculated using numerical integration of the far-field intensity based on Wallace [2]. At the same time, the result of the average radiation efficiency from equation (3.25) is compared with those from the approximate expressions of Maidanik and Leppington.

By applying the given parameters and material of a particular plate, the calculations were carried out for this example rather than using non-dimensional parameters. However, the result can still be used as a guideline for general application.

Two sorts of plate are considered: rectangular plates with sides of similar length and very narrow rectangular plates. The latter is called a strip in the present report. The material is chosen as aluminium. The damping loss factor is assumed to be 0.1 unless otherwise stated. The rectangular plate is 0.5×0.6m, while the strip is 0.16×3m. In both cases the thickness is 0.003m. The calculations are carried out at 121 points in the frequency range between 10Hz and 10kHz.

Figure 3.2 presents the average spatial mean square velocity from equation (3.26) and the average spatial mean square velocity for each mode from equation (3.23) for the rectangular plate. The infinite numbers of modes in these two equations are truncated to a finite number. In

this truncation, at least all modes with natural frequencies below the critical frequency are taken into account. For the current rectangular plate, all modes below 10kHz are included in the calculation.

Figure 3.3 presents the modal and average radiation efficiency of the rectangular plate. It can be seen that below 70Hz the radiation efficiency of the first mode determines the overall result. This is due to the dominance of this mode in the response, see Figure 3.2, and its high $\sigma_{mn}$.

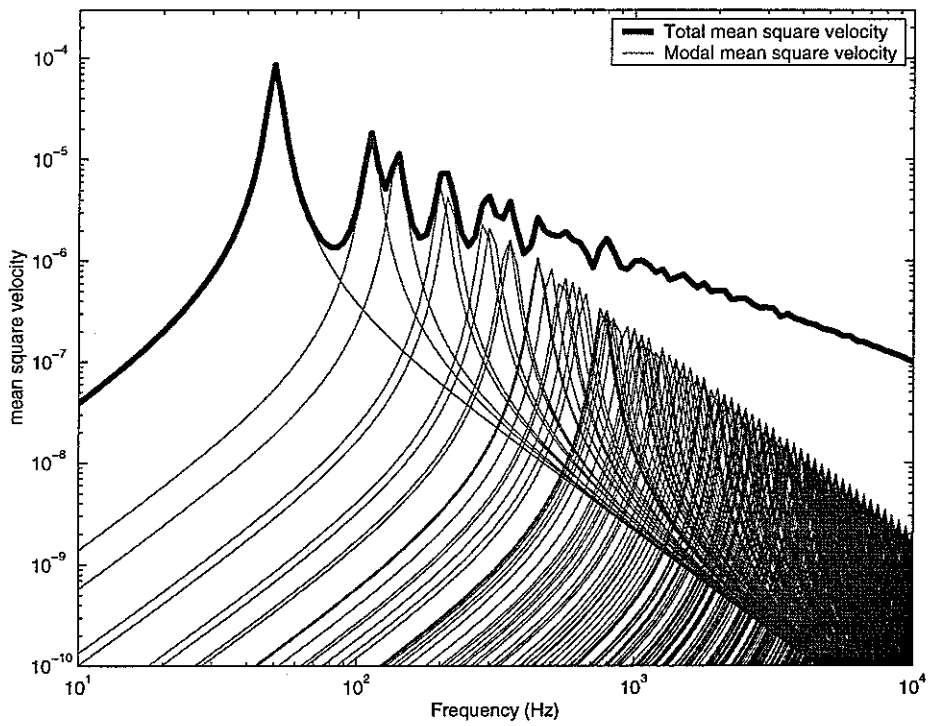


**Figure 3.2 Average mean square velocity of rectangular plate showing contribution from modes ($0.6 \times 0.5 \times 0.003$m aluminium plate with $\eta = 0.1$)**

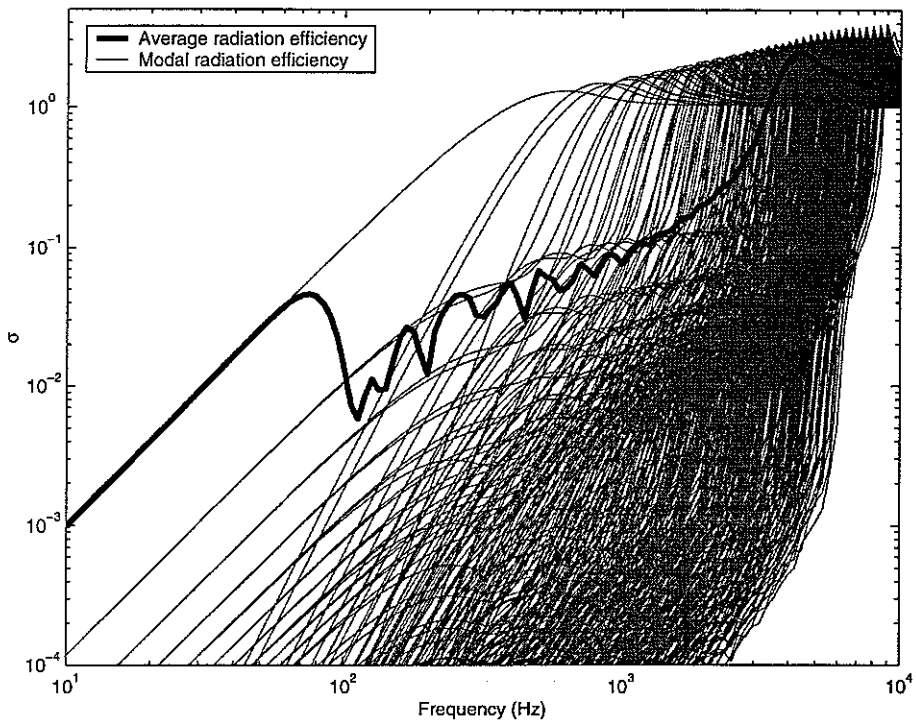


**Figure 3.3 Modal and average radiation efficiency of rectangular plate.**
**($0.6 \times 0.5 \times 0.003$m aluminium plate with $\eta = 0.1$)**

Figure 3.4 presents also the results from the formulae of Maidanik [1] and Leppington [6]. The comparison shows that Maidanik's formula has a good agreement with the numerical result at frequencies well below the fundamental mode of the plate and well above the critical frequency. Between the fundamental natural frequency and the critical frequency, Maidanik's formula mostly underestimates the average radiation efficiency. It is well known that this range is dominated by corner and edge modes. This underestimate is also shown in the experiment by Crocker and Price [17]. It is actually caused because without including the near-field radiation, which will be discussed later in section 3.3. Leppington's formula only gives a good agreement at and well above the critical frequency. For frequencies dominated by edge modes, Leppington's formula agree well with Maidanik's. A poor agreement can be seen for frequencies at and below the fundamental frequency, for which it is not intended.

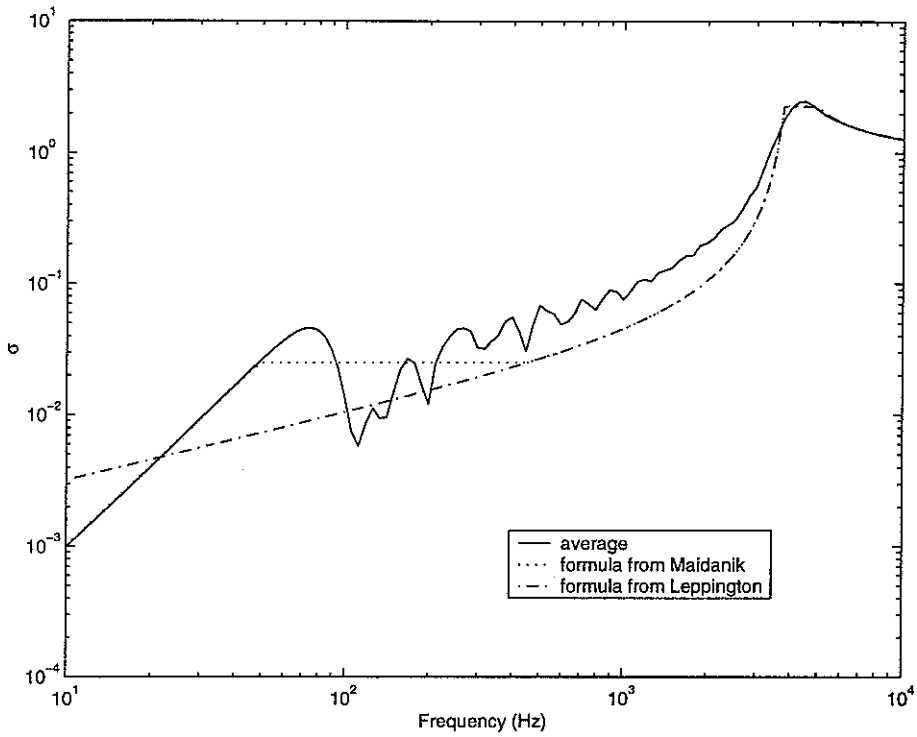


**Figure 3.4 Average radiation efficiency of rectangular plate.**
**($0.6 \times 0.5 \times 0.003$m aluminium plate with $\eta = 0.1$)**

Figure 3.5, Figure 3.6 and Figure 3.7 present the corresponding results for the case of the strip. All modes up to the critical frequency 3980Hz are included. Because of the modal truncation the average mean square velocity in Figure 3.5 falls above about 6kHz.

It can be noted from Figure 3.7 that neither Maidanik's nor Leppingon's formula gives an acceptable estimation. Maidanik's formula only has good agreement with the modal summation results well above the critical frequency. Leppington's formula gives a better estimation at the critical frequency. At the critical frequency, Maidanik's result is too high as indicated by Leppington for a plate with a large aspect ratio [6]. Both estimations give a poor result for frequencies well below the fundamental natural frequency (Leppington's result is not intended to be used in this region). The curve of average radiation efficiency of the strip has two broad peaks, at the fundamental mode (1, 1) and at the second mode along the short edge (2, 1). This requires a further investigation of the radiation behaviour of such a very narrow rectangular plate.

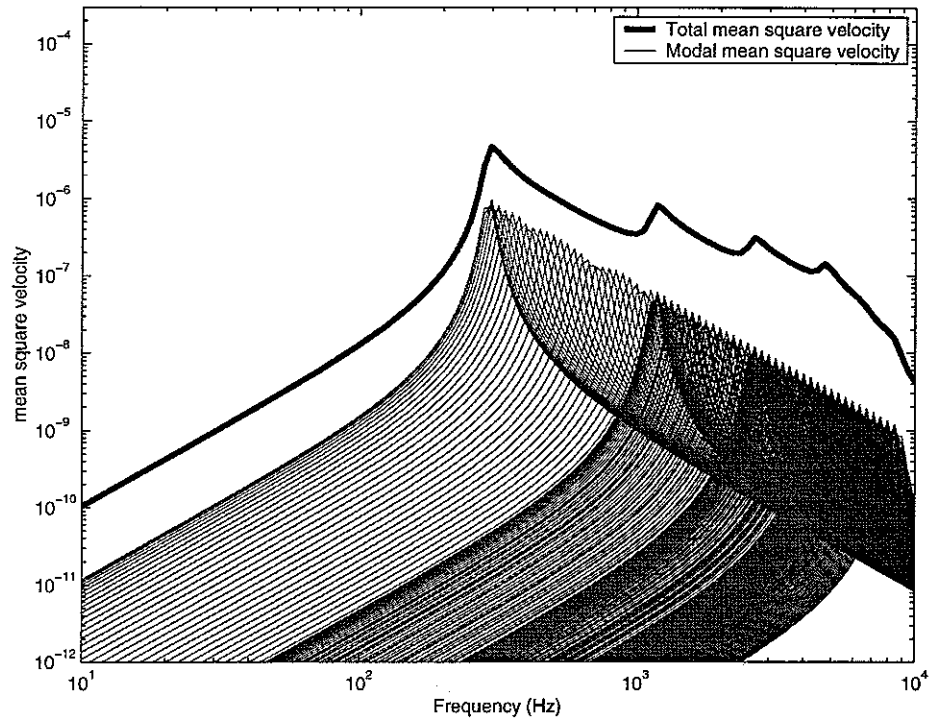


**Figure 3.5 Average mean square velocity of the strip showing contributions from modes.**

**($0.16 \times 3 \times 0.003$m aluminium strip with $\eta = 0.1$)**

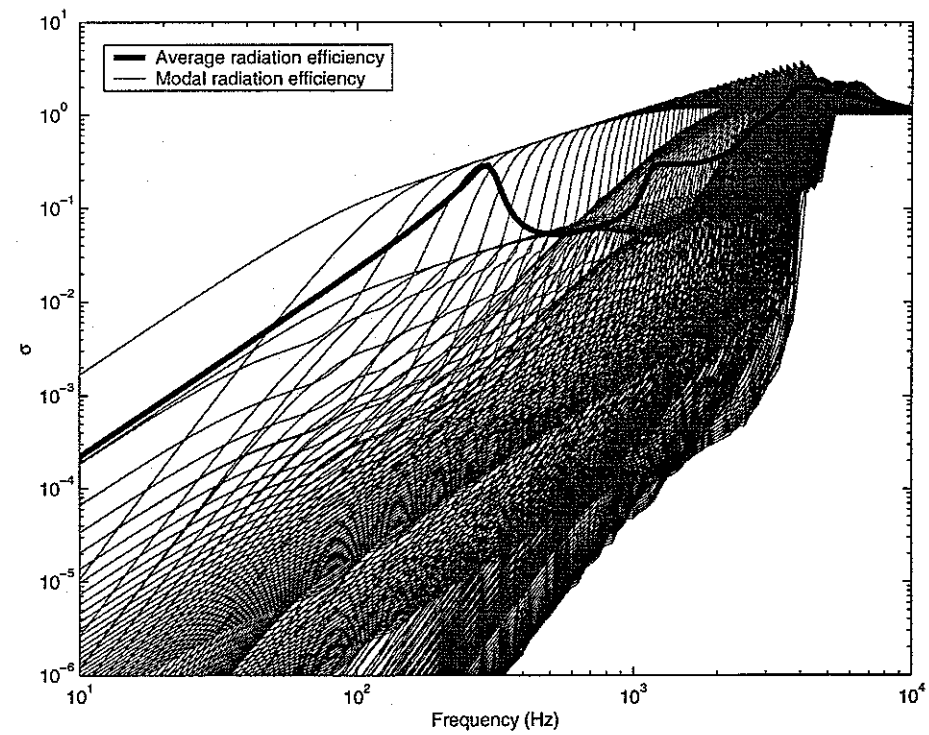


**Figure 3.6 Modal and average radiation efficiency of the strip.**

**($0.16 \times 3 \times 0.003$m aluminium strip with $\eta = 0.1$)**

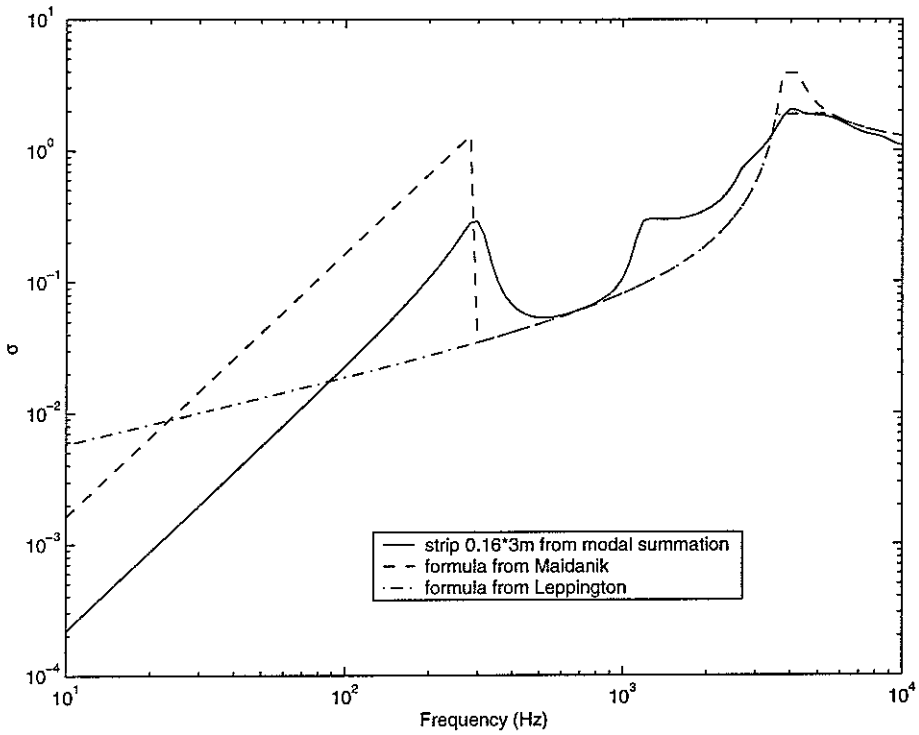


**Figure 3.7 Average radiation efficiency of the strip. (0.16 × 3 × 0.003m aluminium strip with $\eta = 0.1$)**

Maidanik's and Leppington's formulae are based on the assumptions that the plate has a high modal density even in a narrow frequency band and that there is equipartition of modal energy. The first of these conditions requires that the natural modes of the plate are distributed evenly in the $k$-space of the plate. Mathematically, Leppington's model is based on considering a continuous function of the structural wavenumbers. For a rectangular plate, the aspect ratio of which is not too large, this condition can be satisfied approximately. However, this will not be true for the case of a strip. For instance, the strip 0.16×3m has a very sparse distribution of the modes in $k$-space. This is illustrated in Figure 3.8. For a particular frequency band, shown between $k_1$ and $k_2$, the rectangular plate has the characteristics of a nearly equal distribution of the modes. The modes in a band are also distributed between the 'corner' modes and 'edge' modes. The corner modes are referred to those modes whose effective radiating zone is on corners of the plate while edge mode's is on two opposite edges (edge modes are leaded close to the $k_x$ and $k_y$ axes). For the strip, however, the modes in some frequency band may all be 'edge' modes or 'corner' modes.

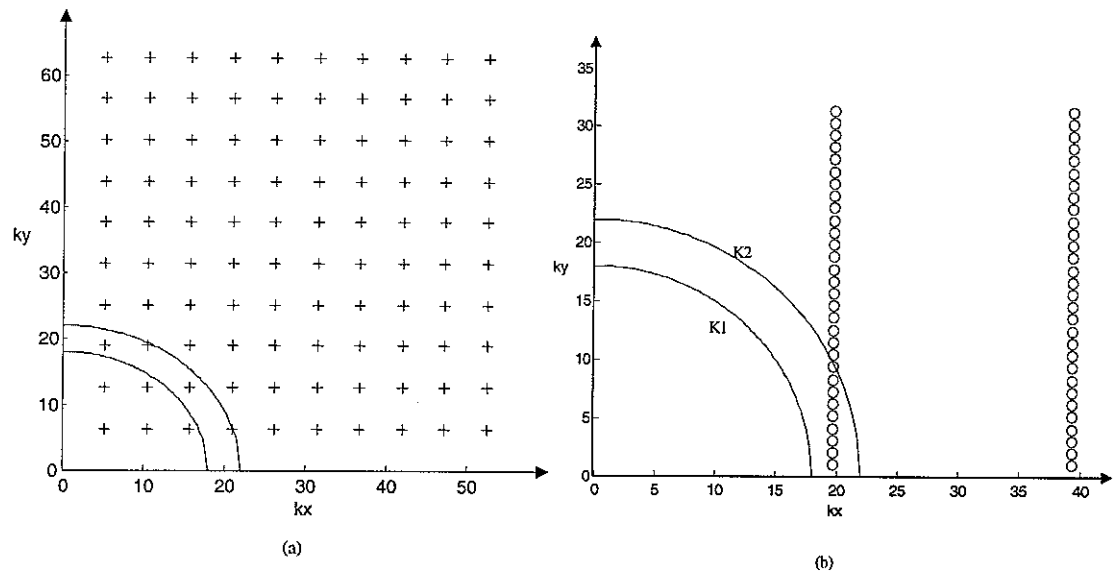


**Figure 3.8 Illustration of the modes in *k*-space. (a) rectangular plate (b) strip**

## 3.2 BELOW THE FUNDAMENTAL MODE

The odd-odd modes are the most effective radiators for a rectangular plate when $ka$, $kb << 1$. For the frequencies well below the fundamental natural frequency, the average radiation efficiency of the plate is dominated by the fundamental mode (see Figure 3.3). This is not only because the radiation of the fundamental mode is most effective. The amplitude of its velocity is also dominant (see equation (3.23) and Figure 3.2). The summation of both the denominator and numerator of equation (3.25) is dominated by the term corresponding to the fundamental mode. Therefore the average radiation efficiency of the plate below the fundamental natural frequency can be given by

$$\sigma \simeq \frac{\sigma_{1,1} u_{1,1}^2}{u_{1,1}^2} = \sigma_{1,1} \tag{3.31}$$

The physical explanation of equation (3.31) is that the whole surface of the plate vibrates in phase in the form of the first mode and the plate motion radiates sound as a monopole.

However, the case of a strip is different from a rectangular plate because of the large aspect ratio. The result of a large aspect ratio is that many modes are distributed closely just above the fundamental frequency (see Figure 3.5). From equation (3.23), it can be seen that the mean square velocity of these modes will have very similar amplitude as $\omega_{mn}$ is similar in each case. As a result, the approximation of equation (3.31) will not be valid anymore. Supposing $p$ modes

contribute to the average radiation efficiency well below the fundamental frequency, equation (3.25) should be rewritten as

$$\sigma \simeq \frac{\sum_{n=1}^{p} \sigma_{1,n} u_{1,n}^2}{\sum_{n=1}^{p} u_{1,n}^2} \tag{3.32}$$

Since the fundamental mode is the most effective in sound radiation (see Figure 2.1), the numerator of equation (3.32) is still dominated by the term corresponding to the fundamental mode. Thus equation (3.32) can be simplified as

$$\sigma \simeq \frac{\sigma_{1,1} u_{1,1}^2}{\sum_{n=1}^{p} u_{1,n}^2} \tag{3.33}$$

It is now necessary to find out which modes of the strip will contribute to the average radiation efficiency. Considering light damping for the plate, the mean square velocity of the mode ($m$, $n$) can be approximated by

$$\overline{\langle u_{m,n}^2 \rangle}(\omega) = \frac{\omega^2 F^2}{2M^2} \frac{1}{\left(\omega_{m,n}^2 - \omega^2\right)^2} \simeq \frac{\omega^2 F^2}{2M^2 \omega_{m,n}^4} \qquad \text{for } \omega \ll \omega_{mn} \tag{3.34}$$

The ratio of the mean square velocity of the mode (1, $n$) to that of the fundamental mode is given by

$$\frac{u_{1,n}^2}{u_{1,1}^2} = \left(\frac{\omega_{1,1}}{\omega_{1,n}}\right)^4 \tag{3.35}$$

where $\omega_{1,1} = \sqrt{\frac{B}{m''}}\left[\left(\frac{\pi}{a}\right)^2 + \left(\frac{\pi}{b}\right)^2\right]$, $\omega_{1,n} = \sqrt{\frac{B}{m''}}\left[\left(\frac{\pi}{a}\right)^2 + \left(\frac{n\pi}{b}\right)^2\right]$.

With $\Delta k_x = \pi/a$ and $\Delta k_y = \pi/b$. Equation (3.35) can be rewritten as

$$\frac{u_{1,n}^2}{u_{1,1}^2} = \left(\frac{\Delta k_x^2 + \Delta k_y^2}{\Delta k_x^2 + n^2 \Delta k_y^2}\right)^4 \tag{3.36}$$

For the case of a strip, $a << b$, $\Delta k_y << \Delta k_x$ and writing $\gamma = a/b$, thus

$$\frac{u_{1,n}^2}{u_{1,1}^2} \simeq \left(\frac{\Delta k_x^2}{\Delta k_x^2 \left(1 + \gamma^2 n^2\right)}\right)^4 \tag{3.37}$$

$$\frac{u_{1,n}^2}{u_{1,1}^2} \simeq \left(1+\gamma^2 n^2\right)^{-4} \tag{3.38}$$

The average radiation efficiency of the strip below the fundamental mode can be rewritten as

$$\sigma = \frac{\sigma_{1,1} u_{1,1}^2}{\sum_{n=1}^{p} u_{1,1}^2 \left(1+\gamma^2 n^2\right)^{-4}} = \frac{\sigma_{1,1}}{\sum_{n=1}^{p} \left(1+\gamma^2 n^2\right)^{-4}} \tag{3.39}$$

It is found by numerical evaluation that $\sum_{n=1}^{p} \left(1+\gamma^2 n^2\right)^{-4}$ can be approximated as

$$\sum_{n=1}^{p} \left(1+\gamma^2 n^2\right)^{-4} \simeq 0.485\left(\frac{1}{\gamma}-1\right) \qquad \text{for } p \text{ large and } \gamma \leq 0.5 \tag{3.40}$$

Then the substitution of equation (3.40) into equation (3.39) gives

$$\sigma \simeq \frac{\sigma_{1,1}}{0.485\left(\frac{1}{\gamma}-1\right)} \tag{3.41}$$

It can be noted that the average radiation efficiency of the strip depends on the aspect ratio and the radiation efficiency of the fundamental mode. Compared with the rectangular plate with the same area, the strip radiates less sound. In order to understand the characteristics of the strip radiation physically, it is instructive to simplify equation (3.41) further as

$$\sigma \simeq \frac{\gamma}{0.485}\sigma_{1,1} \quad \text{for } \gamma \leq 0.1 \tag{3.42}$$

From equation (2.2), the radiation efficiency of the fundamental mode for frequencies well below the fundamental natural frequency can be approximately given by

$$\sigma_{1,1} = \frac{32(ka)(kb)}{\pi^5} = \frac{128}{\pi^3 c^2} abf^2 \tag{3.43}$$

This is proportional to the area of the plate. For the case of the strip, equation (3.42) gives

$$\sigma \simeq \frac{1}{0.485}\frac{a}{b}\frac{128}{\pi^3 c^2} abf^2 = \frac{264}{\pi^3 c^2} a^2 f^2 \simeq \frac{8.5}{c^2} a^2 f^2 \tag{3.44}$$

The average radiation efficiency of the strip at frequencies well below the first mode is thus found to be approximately proportional to the square of the short edge length of the strip and is independent of the long edge length.

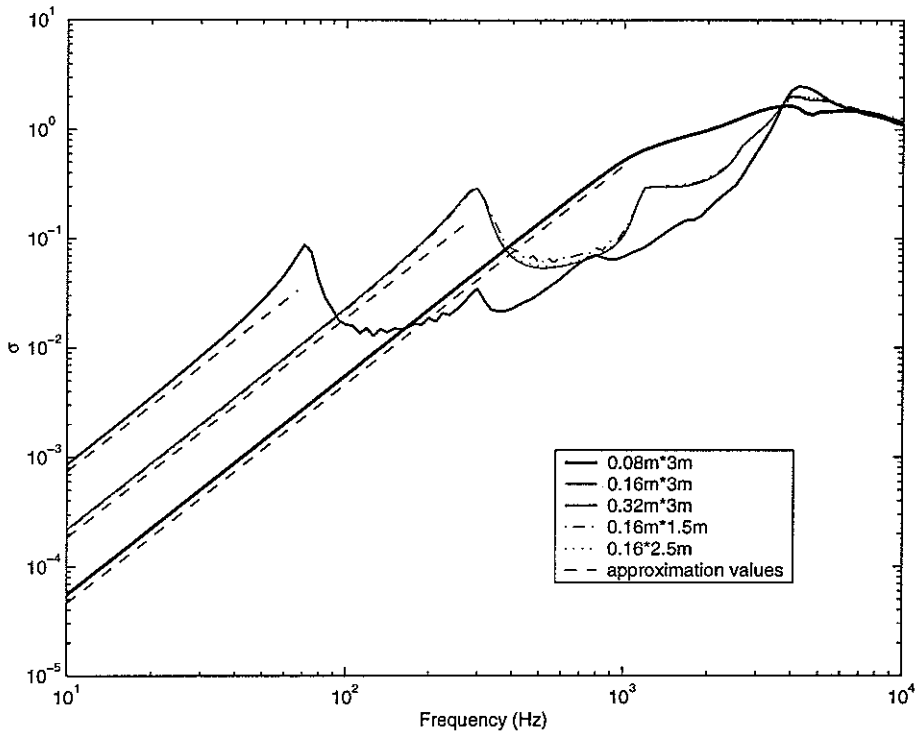


**Figure 3.9 Average radiation efficiency of strips by numerical integration. (aluminium strip with $\eta = 0.1$)**

In order to verify this conclusion, three strips with different aspect ratio are investigated by using a MATLAB program based on equation (3.25) and the modal radiation efficiency from the numerical integration. The short edge is 0.16m and the long edges are 1.5m, 2.5m and 3m respectively. Two other strips with the same long edge 3m but different short edges 0.08m and 0.32m are investigated as well. The results are presented in Figure 3.9. It is seen that the three strips with the same width 0.16m have very similar average radiation efficiencies and are indistinguishable at low frequency. The results also show that the average radiation efficiency below the fundamental mode is proportional to the square of the short edge length of the strip. Equation (3.44) underestimates the average radiation efficiency slightly at low frequency if compared with the results from numerical calculations. This is because of the simplification from equation (3.32) to (3.33) by ignoring the contributions of other modes in the numerator. From Figure 2.1 (also Figure 3.6), it can be seen that mode (1, 3) still has a considerable contribution to the frequencies below the fundamental frequency.

## 3.3 EFFECT OF DAMPING

Different values for the damping loss factor in equation (3.23) and (3.26) are used to calculate the average radiation efficiency based on equation (3.25). The previous example of a rectangular

plate 0.6×0.5m is considered first. Figure 3.10 presents the average radiation efficiency obtained with various damping values. It can be seen that the average radiation efficiency decreases as the modal damping is increases in the frequency range around the critical frequency, and, conversely, increases between the fundamental natural frequency and the critical frequency. It is independent of the damping for frequencies below the fundamental natural frequency and well above the critical frequency.

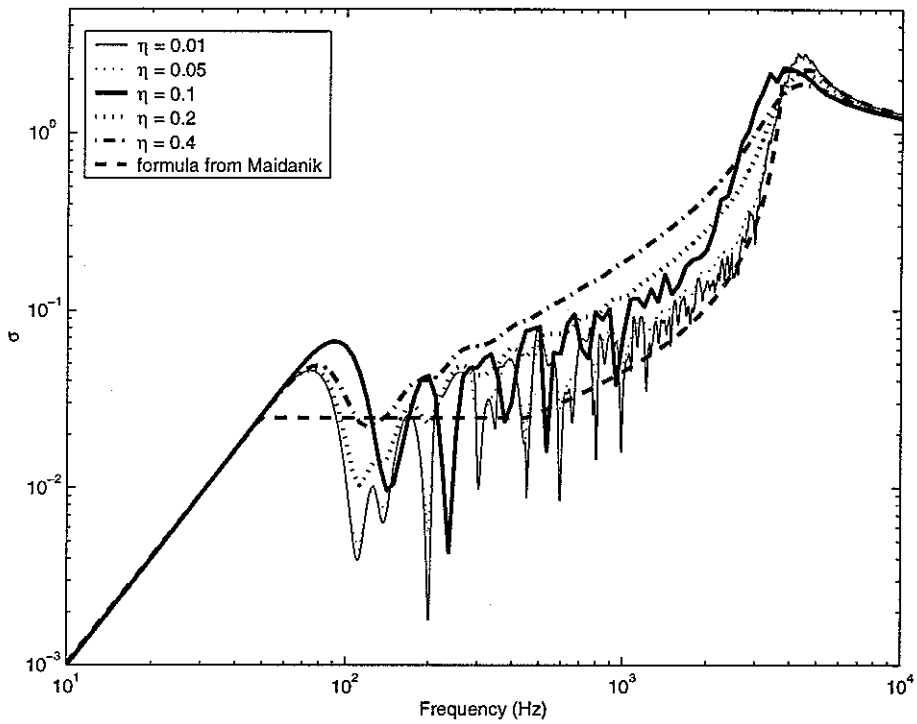


**Figure 3.10 Average radiation efficiency of rectangular plate with various damping ($0.6 \times 0.5 \times 0.003$m aluminium plate)**

This can be understood qualitatively in terms of the modal summation approach used to calculate the average radiation efficiency. Due to the increase in the damping, the amplitude of the modal response at resonance to a point force decreases. So does the spatially averaged mean square velocity. However, away from the resonance frequency the amplitude of the modal response is not affected by the modal damping. Hence, relatively more modes will contribute significantly to the response at any frequency between the fundamental natural frequency and the critical frequency so that the average radiation efficiency increases in this range. For frequencies well below the fundamental natural frequency the modal response is insensitive to the change of damping so that the average radiation efficiency is still dominated by the fundamental mode. For frequencies around the critical frequency, the average radiation efficiency decreases.

An alternative way of understanding the effects of the damping for frequencies between the fundamental natural frequency and the critical frequency is to consider the radiation from the flexural near-field around the excitation point. The total radiation by a highly damped plate consists of contributions from the near-field and from edges. The power radiated by the near-field around the excitation point is given by [16, 18]

$$W_{nf} = \frac{\rho \overline{P}^2}{2\pi c (\rho_s h)^2} \tag{3.45}$$

where $\overline{P}$ is the r.m.s value of the force applied.

This indicates that the power generated by the excitation of a highly damped finite plate, below the critical frequency, is independent of frequency and plate bending stiffness. The total power radiated from these two contributions is hence given by

$$W = \frac{\rho \overline{P}^2}{2\pi c (\rho_s h)^2} + \rho cab\sigma_0 \left\langle \overline{u^2} \right\rangle \qquad \text{for} f < f_c \tag{3.46}$$

where $\sigma_0$ is the radiation efficiency of the multi-modal vibration from the light damped plate, which is given by Maidanik and Leppington.

Using the relation between exciting force and mean-square velocity from the balance between the power input and dissipated:

$$\frac{\overline{P}^2}{8\sqrt{\rho_s h B}} = \omega \eta m \left\langle \overline{u^2} \right\rangle \tag{3.47}$$

and substituting $f_c = \frac{c^2}{2\pi}\sqrt{\frac{\rho_s h}{B}}$, equation (3.46) can be rewritten as

$$W = \rho cab \left\langle \overline{u^2} \right\rangle \left( \frac{4}{\pi} \frac{f}{f_c} \eta + \sigma_0 \right) \qquad \text{for} f < f_c \tag{3.48}$$

This gives an expression for the radiation efficiency of a highly damped plate below the critical frequency as

$$\sigma = \left( \frac{4}{\pi} \frac{f}{f_c} \eta + \sigma_0 \right) \qquad \text{for} f < f_c \tag{3.49}$$

The results from equation (3.49) are compared with those from the modal summation approach and a good agreement is obtained. This is shown in Figure 3.10. The three thin dot lines correspond to the three damping loss factor used in this calculation respectively.

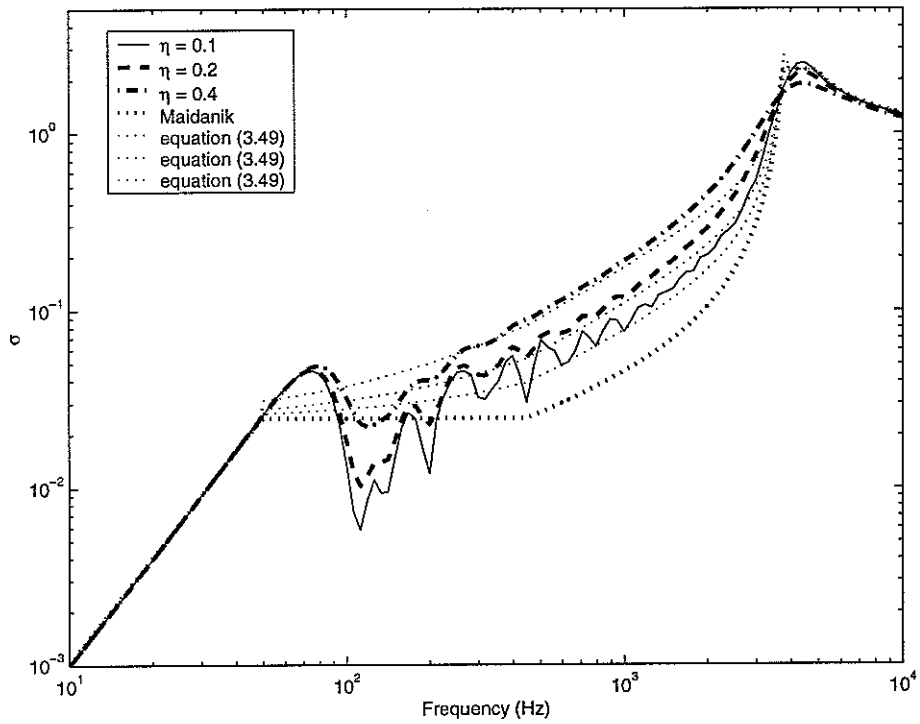


**Figure 3.11 Comparison of the average radiation efficiency between the modal summation and equation (3.49)**

For a highly damped plate with a damping loss factor larger than 0.01, Leppington's formula would underestimate the average radiation efficiency as Maidanik's does. In most practical cases of vibration of lightly damped plates, it can be suggested that either formula is a good approximation for the average radiation efficiency for frequencies between the fundamental frequency and the critical frequency. Considering the effect due to damping, the contribution from the near-field around the excitation point should be taken into account. In such cases, equation (3.49) can give a good estimate.

For the case of strip, the average radiation efficiency is also calculated for various damping values. Figure 3.12 presents the results for the same example strip considered previously. These results are presented in one-third octave bands for clarity. The phenomenon seen above, that the average radiation efficiency is independent of damping for frequencies below the fundamental natural frequency is also seen for the strip. A smaller change than in the case of rectangular plate

can be observed around the critical frequency. However, the average radiation efficiency between the fundamental natural frequency and the critical frequency increases with an increase of damping. A quite large change occurs for the frequencies between the first two cut-on frequencies, where the radiation efficiency appears to be proportional to the damping loss factor.

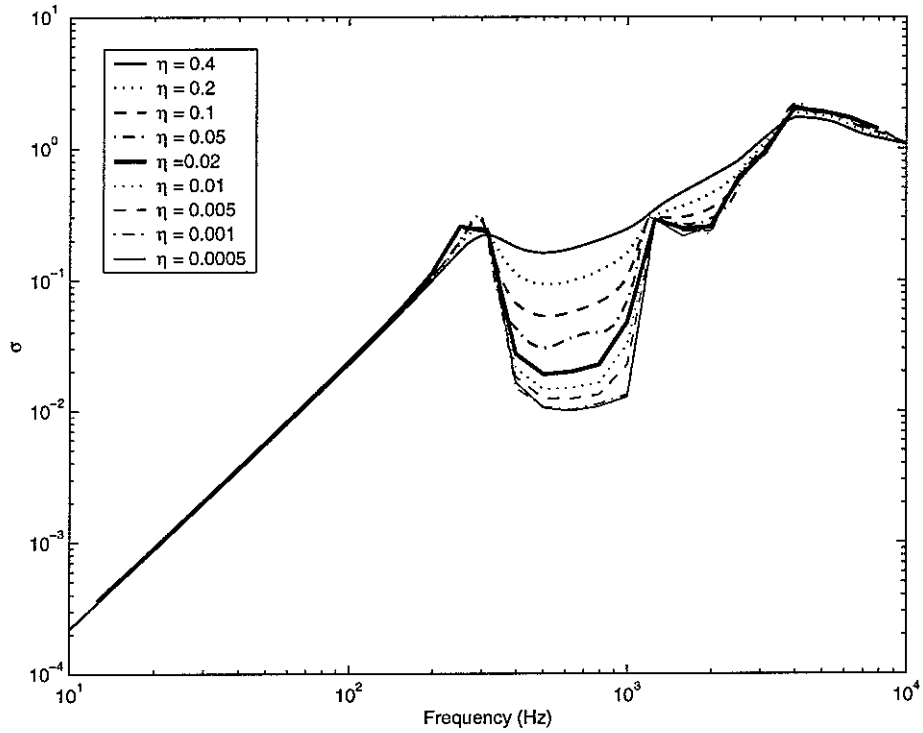


**Figure 3.12 Average radiation efficiency of strip with various damping ($0.16 \times 3 \times 0.003$m aluminium plate)**

The radiation efficiency at 630Hz for different values of the damping loss factor is presented in Figure 3.13. Equation (3.49) is also calculated for damping loss factors of 0.1, 0.2 and 0.4 to compare with the corresponding results from the modal summation approach, as shown in Figure 3.14. It is not surprising to obtain a poor agreement since the result from modal summation approach for damping loss factor of 0.1 is close to that from $\sigma_0$ by Maidanik (see also Figure 3.7). The reason causing this disagreement can be attributed qualitatively from both the modal radiation and near-field radiation.

The sparse distribution of the modes in $k$-space results in the assumption of a high modal density not applicable and thus the formulae for calculating $\sigma_0$ by Maidanik and Leppington are not applicable. This can be represented in a comparison of wavenumber between the acoustical and structural, as shown in Figure 3.15. For frequencies in the middle between the fundamental and

second cut-on natural frequencies, corresponding to $k_{a2}$ for acoustical wavenumber and $k_{b2}$ for structural one, the radiation is basically controlled by corner modes. Thus relatively low radiation efficiencies occur around this frequency. For frequencies close to either the fundamental or second cut-on natural frequency, corresponding to $k_{a1}$, $k_{a3}$ for acoustical wavenumber and $k_{b1}$, $k_{b3}$ for structural one, the radiation is controlled mainly by edge modes. This causes two broad peaks around these two frequencies. For frequencies above the second cut-on frequency, the distribution of modes tends to an even one so that the disagreement gradually decreases as frequency increases.

The characteristic of the near-field radiation also appears different from the case of rectangular plates. By comparing the radiation efficiency at 630Hz between the rectangular plate and the strip, it is found that the varying rate of the radiation efficiency for the strip as the damping changes is approximately two times of that for the rectangular plate. This is shown in Figure 3.13.

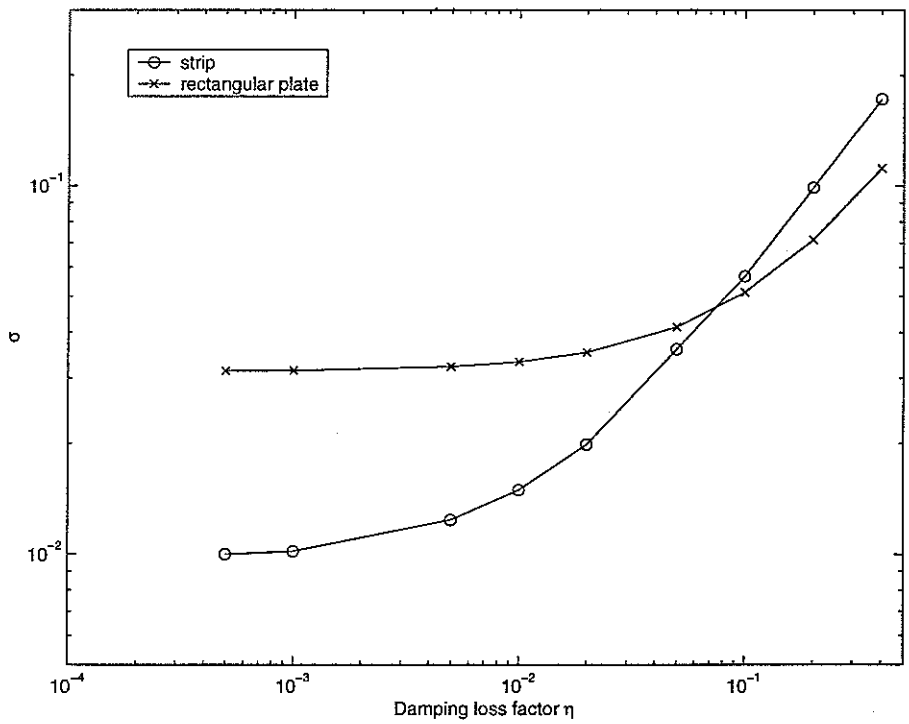


**Figure 3.13 Radiation efficiency at 630Hz with various damping.**

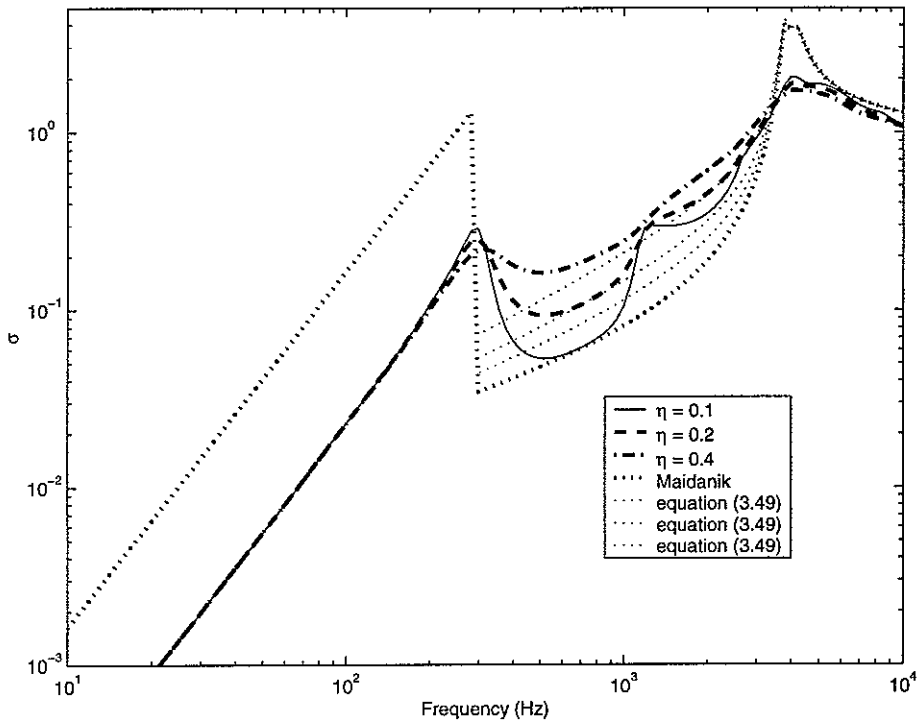


**Figure 3.14 Comparison of the average radiation efficiency for strip between the modal summation and equation (3.49)**

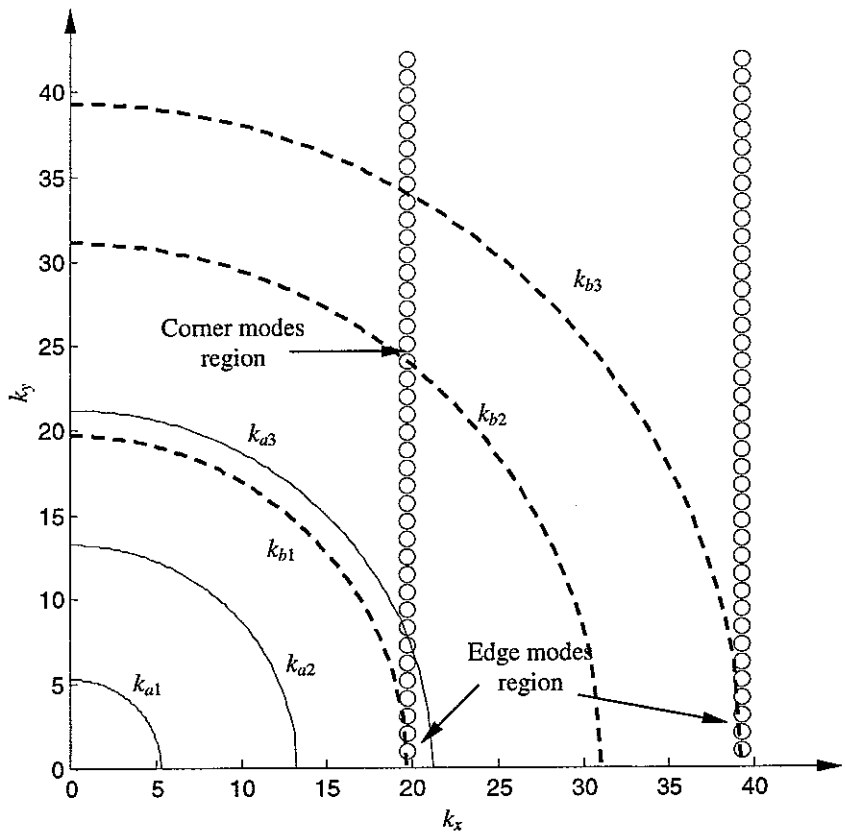


**Figure 3.15 Comparison of acoustical and structural wavenumber showing the characteristic of the modal radiation of the strip for frequencies between the fundamental and second cut-on natural frequencies.**

For the frequencies between the fundamental natural frequency and the second cut-on frequency, provided $k_x$, $k_y > k_a$, the radiation from the strip can be considered to be equivalent to the radiation of two edge monopoles each of size $a \times \lambda_y/4$ where $\lambda_y$ is the wavelength along the length of the strip. The power radiated by the strip in this region is given by

$$W = 2 \times W_m = 2\rho c S_m \left\langle \overline{v_m^2} \right\rangle \sigma_m \tag{3.50}$$

where $\sigma_m = \dfrac{4f^2 S_m}{c^2}$ is the radiation efficiency of a monopole with the velocity distribution of a simply supported plate. $S_m = a\lambda_y / 4$ is the area of the monopole, and $\left\langle \overline{v_m^2} \right\rangle$ is the mean square velocity within these monopole regions. The radiation efficiency of the whole strip with light damping can thus be given by

$$\sigma_{0s} = \frac{W}{\rho c a b \left\langle \overline{v^2} \right\rangle} = \frac{2\sigma_m S_m}{ab} = \frac{8 S_m^2 f^2}{abc^2} \tag{3.51}$$

since $\left\langle \overline{v_m^2} \right\rangle = \left\langle \overline{v^2} \right\rangle$. Substituting $\lambda_y = 2b/n$, equation (3.51) becomes

$$\sigma_{0s} = \frac{2abf^2}{c^2 n^2} \qquad \text{for } f_{1,1} < f < f_{2,1},\ k_y > k_a \tag{3.52}$$

where $n$ is the index of modes in $y$-direction along the length.

From Figure 3.3, it is found that the dependence of the radiation efficiency for the strip on the damping loss factor is approximately twice that for the rectangular plate. So the near-field radiation efficiency for the strip in this region can be approximated as

$$\sigma_{near} = \frac{8}{\pi} \frac{f}{f_c} \eta \qquad \text{for } f_{1,1} < f < f_{2,1},\ k_y > k_a \tag{3.53}$$

The radiation efficiency of the strip in this region is finally approximately given by

$$\sigma = \sigma_{0s} + \sigma_{near} = \frac{2abf^2}{c^2 n^2} + \frac{8}{\pi} \frac{f}{f_c} \eta \qquad \text{for } f_{1,1} < f < f_{2,1},\ k_y > k_a \tag{3.54}$$

The calculation results from equation (3.54) are compared with the results from the modal summation. Figure 3.16 shows the results for the strip of dimensions $0.16 \times 3$m with values of damping loss factor of 0.0005 and 0.1. Although small errors exist, especially for large damping, equation (3.54) gives a fairly good approximation for this region. For the strip of dimensions $0.32 \times 3$m, the comparison is presented in Figure 3.17. The above model is also shown to be a good approximation for the radiation efficiency in this region.

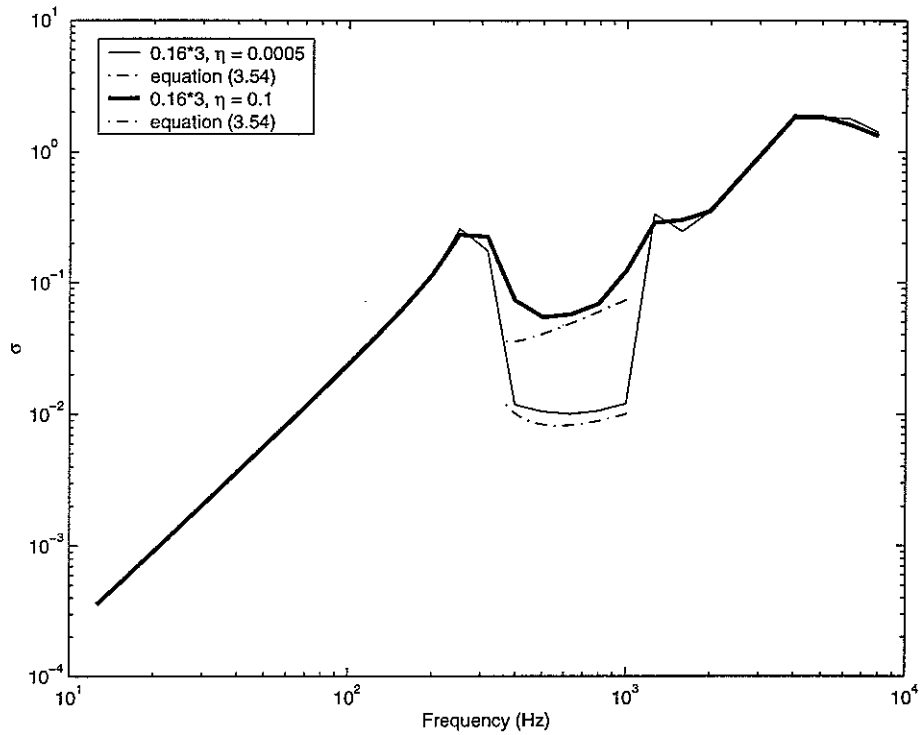


**Figure 3.16 Estimation of the radiation efficiency of the strip 0.16 × 3m for the frequencies between the fundamental and second cut-on natural frequency.**

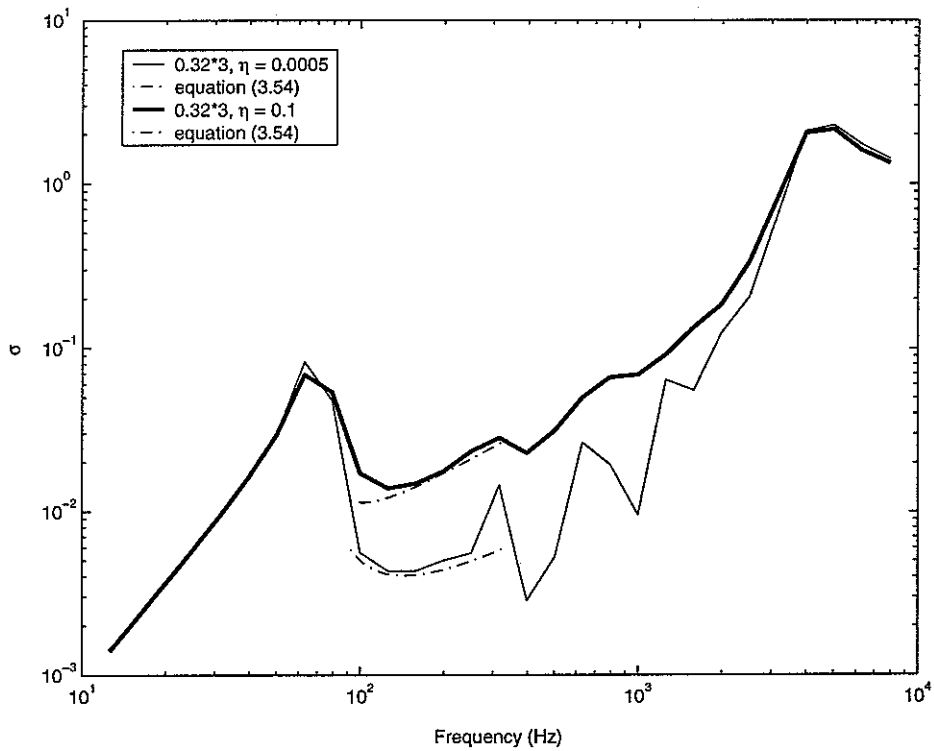


**Figure 3.17 Estimation of the radiation efficiency of the strip 0.32 × 3m for the frequencies between the fundamental and second cut-on natural frequency.**

## 3.4 RADIATION EFFICIENCY AT THE CRITICAL FREQUENCY

For plates with relatively low critical frequencies, both Maidanik's and Leppington's formulae, equation (3.28) and (3.29), will give a value of radiation efficiency for the critical frequency smaller than unity. This corresponds to thick, stiff plates. For example, the character of the radiation of a plate is dominated only by the first mode if its critical frequency is lower than its first natural frequency. In this case, it will be not appropriate to use Mainanik's and Leppington's formulae to consider the radiation behaviour of plates.

Using the modal summation approach, the radiation efficiencies at the critical frequency are reinvestigated and compared with results from Leppington's and Maidanik's formulae. Figure 3.18 presents the radiation efficiencies at critical frequencies with different aspect ratios according to Leppington (see equation (3.29)). The non-dimensional parameter of the product of the wavenumber at the critical frequency and the shortest edge $a_1$ of the plate is used in Figure 3.18. It can be seen that Leppington's formula gives results less than unity for $ka_1$ smaller than a certain value for a certain aspect ratio, eg $ka_1 \approx 7.6$ for $\gamma = 1$, $ka_1 \approx 4.2$ for $\gamma = 0.2$.

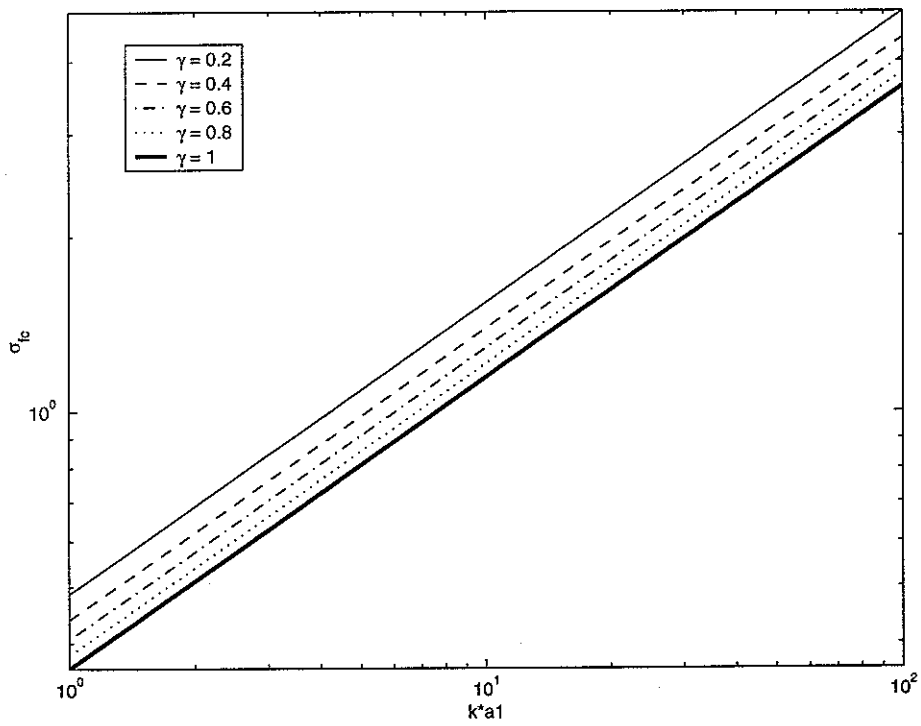


**Figure 3.18 Radiation efficiencies at critical frequencies by Leppington.**

To use the non-dimensional parameter $ka_1$ for Maidanik's formula, the expression for the critical frequency in equation (3.28) is rewritten as

$$\sigma = 0.45(ka_1)^{\frac{1}{2}}\left(\frac{\gamma+1}{\gamma\pi}\right)^{\frac{1}{2}} \tag{3.55}$$

where $a_1$ denotes the length of the shorter edges, $\gamma$ has the same meaning as that in Leppington's formula.

Figure 3.19 presents the corresponding results by Maidanik's formula, which gives results less than unity for $ka_1 \approx 7.6$ for $\gamma = 1$ and $ka_1 \approx 2.6$ for $\gamma = 0.2$.

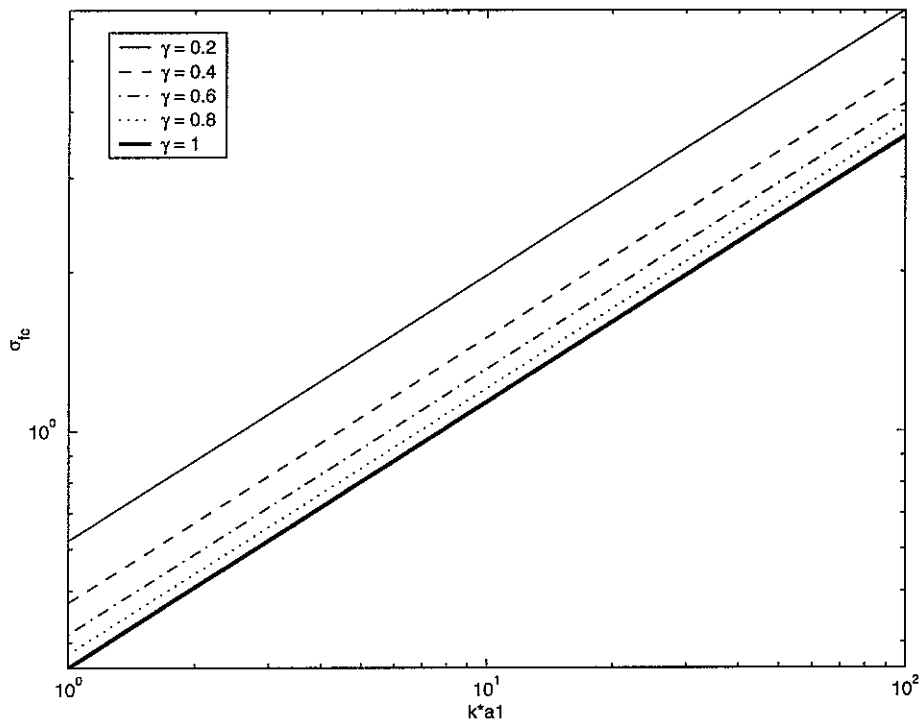


**Figure 3.19 Radiation efficiencies at critical frequencies by Maidanik.**

Figure 3.20 presents a comparison of the results from modal summation and according to Leppington and Maidanik for square plates. The damping loss factor for the plate is 0.01. The results from modal summation are the maximum radiation efficiency which occur arroud or just above the critical frequency. Both narrow band and one-third octave band results from the modal summation are plotted. For large values of $ka_1$, the maximum value from the narrow band results is larger than that from 1/3 octave band. The narrow band results appears to converge with Leppington's approximate result for very large values of $ka_1$, but the result from one-third octave bands is lower than Leppington's at large $ka_1$. For $ka_1$ smaller than 3, the radiation efficiency tends to a constant 1.3 that is actually determined by the radiation effect of the fundamental mode (see Figure 3.3). This constant can be given by equation (2.2) according to Wallace [2]. In

such cases, the plate is either very thick or stiff so that its critical frequency is near or lower than the fundamental natural frequency. For square plates, the Maidanik's result is similar to Leppington's.

Figure 3.21 presents the average radiation efficiencies of square plates with different thickness.

Damping does have certain effects on the results from the modal summation approach. Figure 3.22 presents corresponding results for a damping loss factor of 0.1. The radiation efficiency at the critical frequency will decrease with the increase of damping loss factor for large values of $ka_1$. For $ka_1$ smaller than 10, the radiation efficiency at the critical frequency is largely independent of damping loss factor.

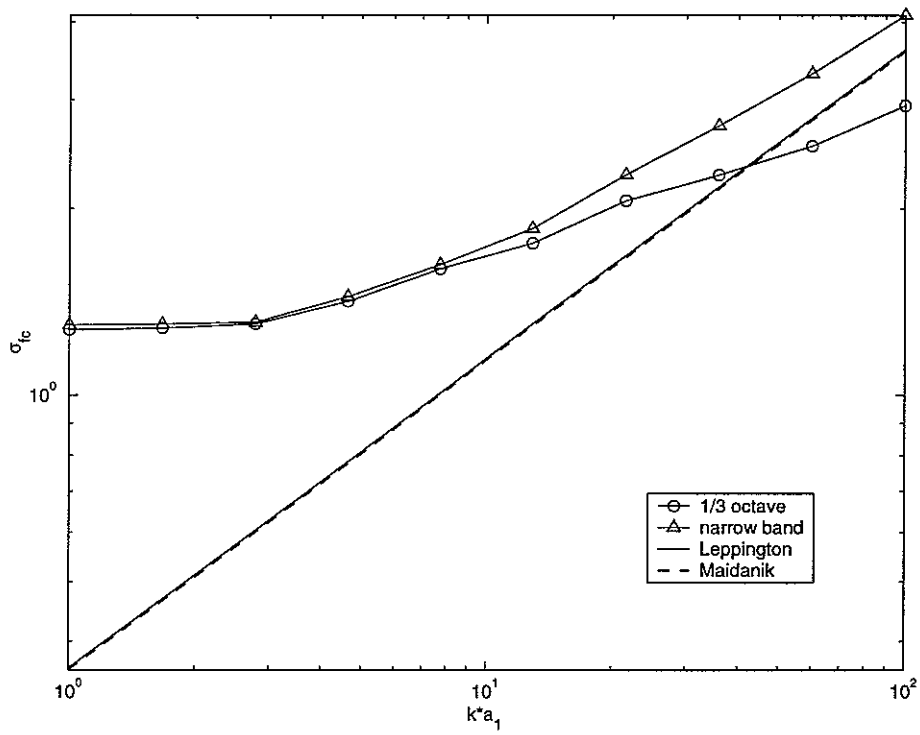


**Figure 3.20 Radiation efficiencies at critical frequencies from modal summation ($\gamma = 1$, damping loss factor 0.01)**

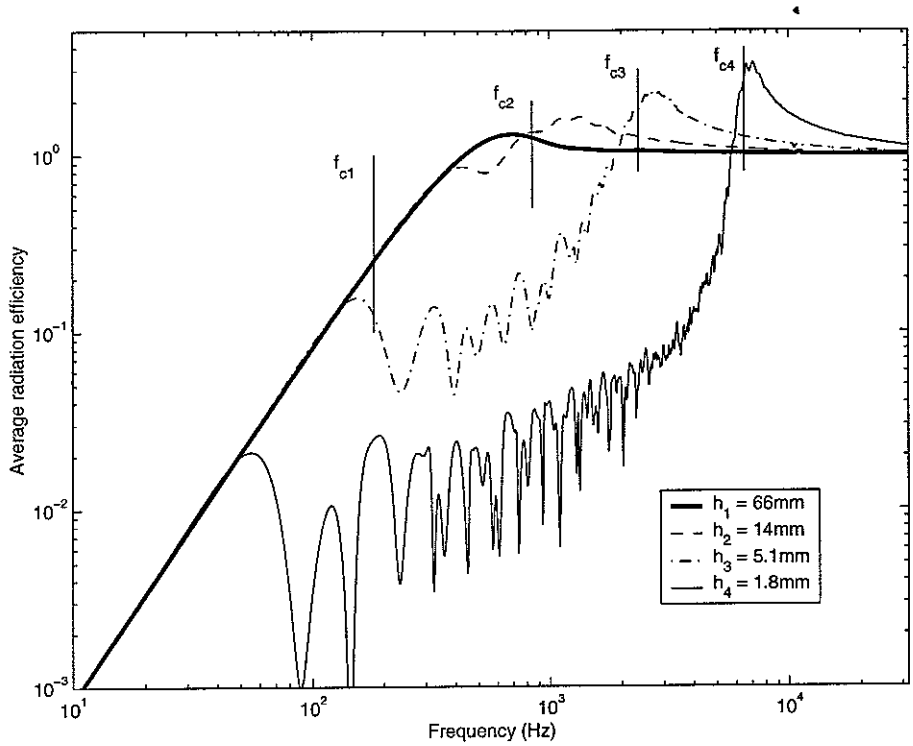


**Figure 3.21 Average radiation efficiency of plate 0.5 × 0.5m with several different thickness**

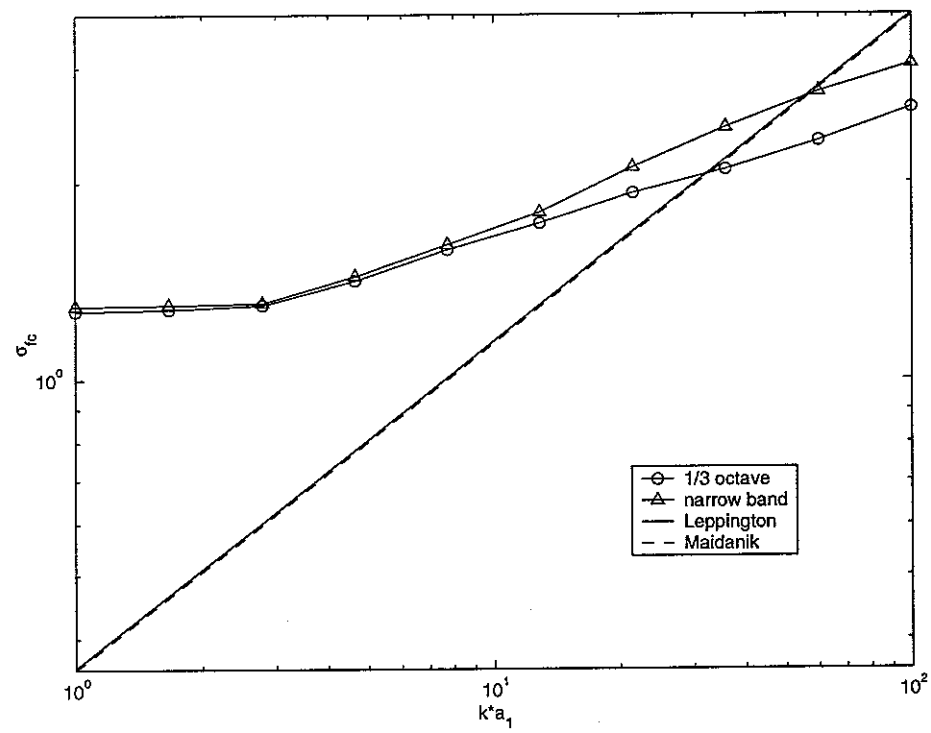


**Figure 3.22 Radiation efficiencies at critical frequencies from modal summation ($\gamma$ = 1, damping loss factor 0.1)**

Corresponding investigations are carried out for a plate with $\gamma = 0.2$. Figure 3.23 presents the comparison of the results from modal summation and formulae by Leppington and Maidanik. A damping loss factor of 0.01 is used in these calculations. For large $ka_1$, Leppington's approximation relatively overestimates the radiation efficiency at the critical frequency compared with the result from the modal summation. For $ka_1$ smaller than 2, the radiation efficiency at the critical frequency tends to a constant 1.2 as before. The one-third octave band result from modal summation has a similar value to Leppington's approximation for $ka_1$ between 20 and 30. Results were not produced for large values of $ka_1$ due to the very long time computation time required.

The result for a damping loss factor of 0.1 is also presented in Figure 3.23. It can be seen that the difference between the result from 1/3 octave bands and narrow bands decreases as damping increases. Maidanik's formula overestimates the radiation efficiency at the critical frequency for narrow plates [6].

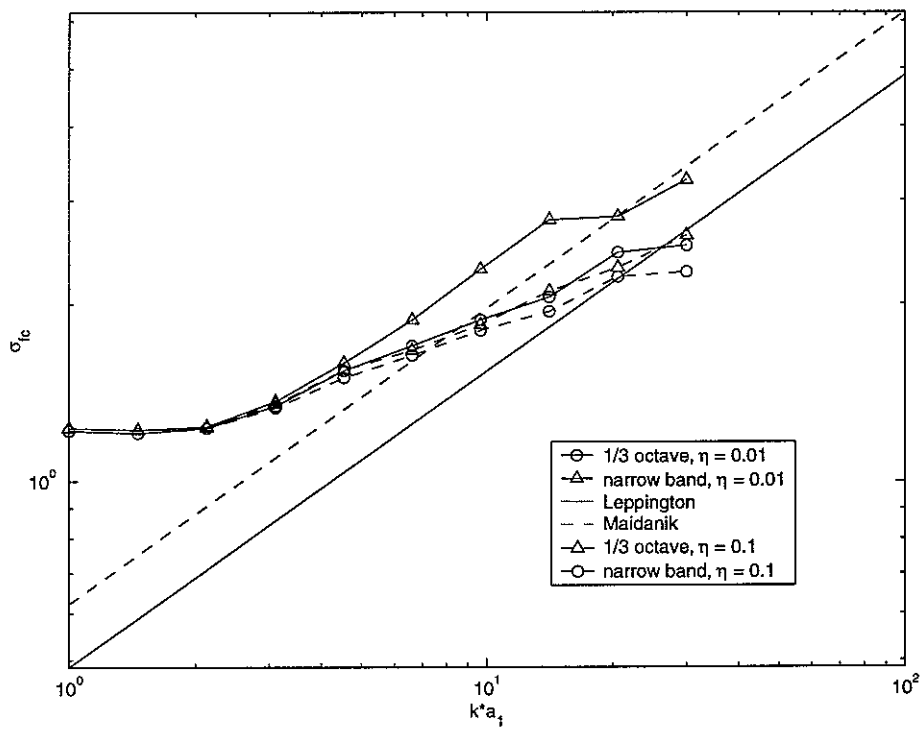


**Figure 3.23 Radiation efficiencies at critical frequencies from modal summation ($\gamma = 0.2$, damping loss factor 0.01 and 0.1)**

In order to find a general relation between the maximum average radiation efficiency and the value of $ka_1$, the analysis is then extended for plates with $\gamma = 0.4$, 0.6 and 0.8. Figure 3.24 shows the results for five different aspect ratios from the modal summation. All data is in one-third octave bands. For $ka_1 < 3$, the radiation efficiency tends to the constant from 1.2 to 1.3 for different aspect ratio, determined by the maximum of equation (2.2) for the fundamental mode. For $ka_1 > 3$, the radiation efficiency increase proportionally with $(ka_1)^{1/4}$, not $(ka_1)^{1/2}$ as Leppington's and Maidanik's. This is given by an approximated expression as

$$\sigma_c = \begin{cases} 1.2 \sim 1.3 & \text{for } ka_1 \le 3 \\ (ka)^{1/4} & \text{for } ka_1 > 3 \end{cases} \tag{3.56}$$

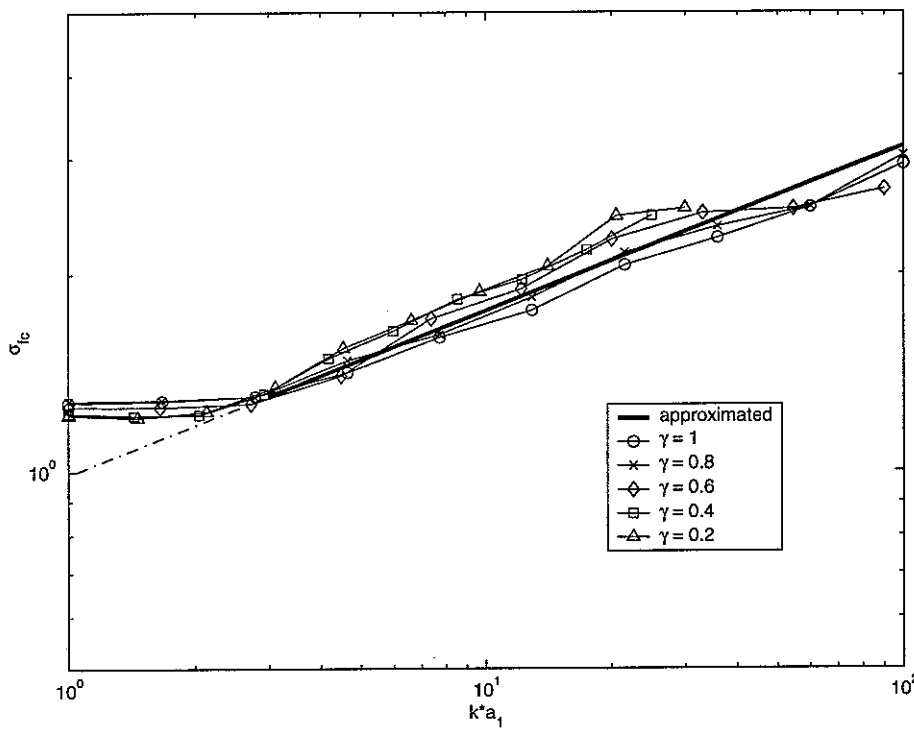


**Figure 3.24 Radiation efficiencies at the critical frequencies from modal summation (in 1/3 octave band) for different aspect ratios.**

## 3.5 CONCLUSIONS

The average radiation efficiency of a rectangular plate due to a point force, including the effect of the damping, can be calculated by using a combined formula from previous results and the present investigations. This is given by

$$\sigma = \begin{cases} \dfrac{4S}{c^2} f^2 & \text{for } f < f_{1,1} \\ \sigma = \left( \dfrac{4}{\pi} \dfrac{f}{f_c} \eta + \sigma_0 \right) & \text{for } f_{1,1} \le f < f_c; \\ \begin{cases} 1.2 \sim 1.3 & \text{for } ka_1 \le 3 \\ (ka)^{1/4} & \text{for } ka_1 > 3 \end{cases} & \text{for } f = f_c \\ \left( 1 - \dfrac{f_c}{f} \right)^{-1/2} & \text{for } f > f_c \end{cases} \tag{3.57}$$

where the expressions below the fundamental mode and above the critical frequency are from Maidanik's formula (see equation (3.28)). The expression from the fundamental mode to the critical frequency is from equation (3.49). And the expression for the critical frequency is from (3.56).

For the rectangular plate with a large aspect ratio ($\gamma$ smaller than 0.1), equation (3.44) can be used to replace the corresponding one in equation (3.57) for frequencies well below the fundamental natural frequency. For frequencies between the fundamental natural frequency and the second cut-on frequency, the radiation efficiency of the strip appears to be proportional to the damping loss factor. In this region, equation (3.54) can be used for estimating the radiation efficiency. For frequencies between second cut-on natural frequency and the critical frequency, the radiation efficiency of the strip can also be approximated with equation (3.49).

# 4 RADIATION OF EXTRUDED PLATES

The radiation of a double-skinned extruded plate is far more complicated than the foregoing discussion of a rectangular plate. Calculation of the radiation efficiency requires a knowledge of the velocity distribution over the surface of the structure which is the case of the extruded plate becomes unwieldy because of the complexity of the structure. The vibration of the extruded plate can be considered to involve global motion and local motion. At low frequencies it behaves as a whole plate while the local vibration of individual strips dominates at high frequencies [13]. The radiation of the extruded plate can therefore be treated in terms of the contributions from both global modes and local modes. By following the foregoing analysis, where an average over all point force excitations over the plate is considered, these global and local modes may be assumed to radiate sound independently of each other by orthogonality of the mode shapes

(strictly speaking they are only orthogonal if mean-normalised and integrated over the whole plate, but the forces are only applied on the outer skin). Therefore, an average radiated power for the extruded plate can be given by

$$\overline{W} = \overline{W}_{global} + \overline{W}_{local} \tag{4.1}$$

where $\overline{W}_{global}$ and $\overline{W}_{local}$ represent the power radiated by global modes and local modes respectively.

The radiation efficiency of the extruded plate can be thus given by

$$\sigma = \frac{\overline{W}_{global} + \overline{W}_{local}}{\rho c A \overline{\langle u^2 \rangle}} \tag{4.2}$$

where $A$ is the surface area of the extruded plate, $\overline{\langle u^2 \rangle}$ is the spatially averaged mean square velocity over one side of the extruded plate and $\overline{W}_{global}$ and $\overline{W}_{local}$ refer to radiation from that side.

In the following sections, the radiation from global modes and local modes of the extruded plate will be discussed under certain assumptions. These will be combined to give an expression for the total radiation efficiency. An example of the extruded plate and the corresponding coordinate system under discussion is illustrated in Figure 4.1.

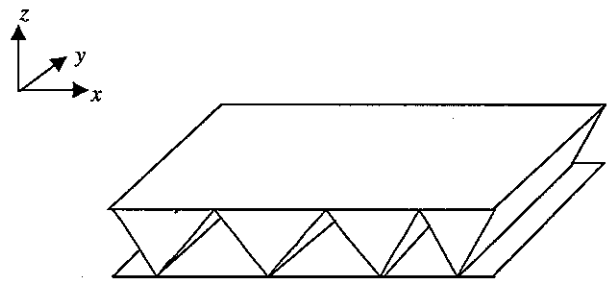


**Figure 4.1 Example of an extruded plate**

## 4.1 RADIATION FROM GLOBAL MODES

### 4.1.1 MODEL FOR GLOBAL MODES

Consider the extruded plate as an equivalent plate in bending vibration, namely global bending motion. In such case, the stiffeners are nearly rigid and the bending induces stresses mainly in the upper and lower plates. The upper or lower plates would be either compressed or extended

relative to the neutral fibre. This neutral fibre passes through the centre of gravity of the section, and actually is located at the mid-point of the section (see Figure 4.2). The stiffeners do not bear the tensile and compressive stress under the pure bending condition and behave as rigid spacers that separate the upper and lower plates.

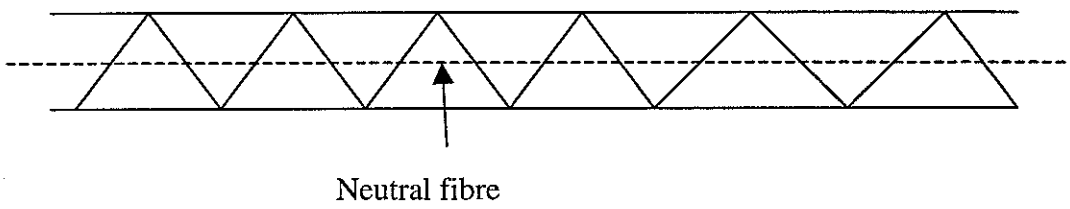


**Figure 4.2 Illustration of the neutral fibre of the extruded section**

Based on the above assumption, the second moment of area about the $y$ axis per unit width can be calculated by [13]

$$I_x = 2\times\left(\frac{h^3}{12}+\left(\frac{H}{2}-\frac{h}{2}\right)^2\times h\right) \tag{4.3}$$

where $h$ is the thickness of the upper and lower plates and $H$ is the overall height of the extruded plate. This is illustrated in Figure 4.3.

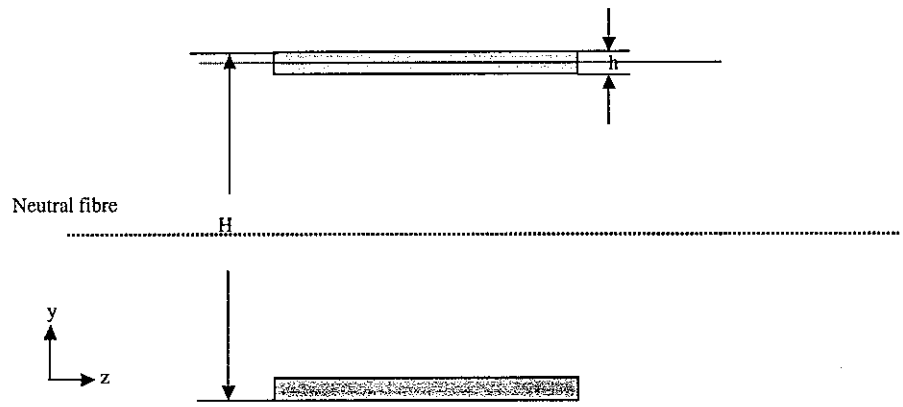


**Figure 4.3 Model for calculating the second moment of area of the cross section**

The equivalent bending stiffness along the $x$ axis can therefore be calculated by

$$B_x = E'I_x = \frac{EI_x}{1-\mu^2} \tag{4.4}$$

where $E$ is the Young's modulus and $\mu$ is the Poisson ratio of the material.

For bending along the $z$ axis, the second moment of area about the $y$ axis based on the above assumption can be considered as an equivalent counterpart of a II section [19], as shown in Figure 4.4. This gives

$$I_y = 2\times\left[\left[\frac{ah^3}{12}+ah\times\left(\frac{H}{2}-\frac{h}{2}\right)^2\right]+\frac{h(H-2h)^3}{12\sin\alpha}\right] \tag{4.5}$$

where $a$ is the average space between the stiffeners.

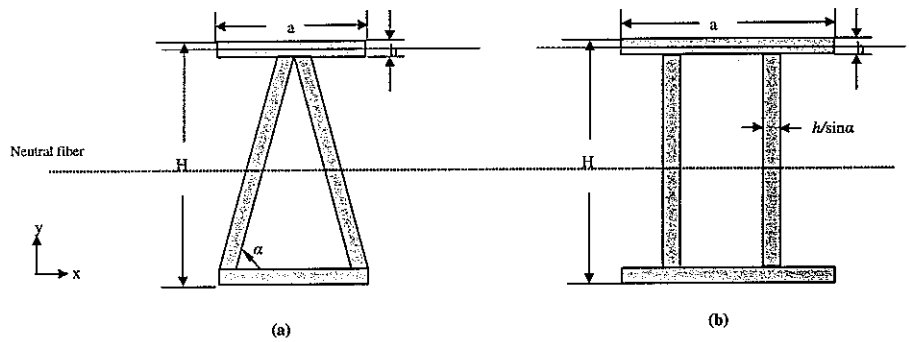


**Figure 4.4 (a) Cross section of part of the extruded plate. (b) The cross-section of the equivalent II section**

The equivalent bending stiffness along the $y$ axis is given by

$$B_y = E'I_y = \frac{EI_y}{1-\mu^2} \tag{4.6}$$

The bending stiffnesses $B_x$ and $B_y$ from equations (4.4) and (4.6) have very similar values since the second moment of area is dominated by the cross-section of the top and bottom plates. $B_x$ is calculated as $5.369\times10^5$ m$^4$ and $B_y$ is $5.715\times10^5$ m$^4$ for a typical section [13]. In spite of this similarity, the extruded plate behaves as an orthotropic plate because its bending stiffness varies with direction. For orthotropic plates, if the bending wavelength is considerably greater than the stiffener spacing, it can be approximated as an equivalent isotropic plate by introducing an equivalent bending stiffness $B_{xy}$ [16]. This equivalent bending stiffness $B_{xy}$ is equal to the geometric mean of the bending stiffness in the two directions. It is given by

$$B_{xy} \approx \sqrt{B_x B_y} \tag{4.7}$$

With such an equivalent isotropic plate, the problem of the radiation from the global modes of the extruded plate can be treated in the same way as that of a rectangular plate discussed in section 3. It should be indicated that the critical frequency behaviour of orthotropic plates, whose

bending stiffness in two directions are largely different, is somewhat more complicated. The bending wavenumbers and thus the wavelengths of such plates depends on the direction of propagation along the plate. In the direction of the greatest stiffness, the corresponding critical frequency is lower than that of the smallest stiffness. There are rather complicated relations between the two critical frequencies [20]. For the present extruded plate under consideration, the critical frequencies in the two directions are very similar due to the similarity of the bending stiffness in the two directions. Hence, the model of the equivalent isotropic plate is accurate enough to be used to study the radiation from the global modes of the extruded plates.

### 4.1.2 AVERAGE RADIATION EFFICIENCY OF GLOBAL MODES

Considering all possible point force locations over the surface of the extruded plate, the average radiation efficiency from global modes can be calculated by using equation (3.25). The modal radiation efficiencies are obtained by using numerical integration in MATLAB. The spatially averaged mean square velocity is given by equation (3.26) based on assuming simply supported boundary conditions.

The example of the extruded plate used in the present report is of aluminium and of dimension 2.016×3.0×0.07m. The critical frequency for the global modes is 139Hz.

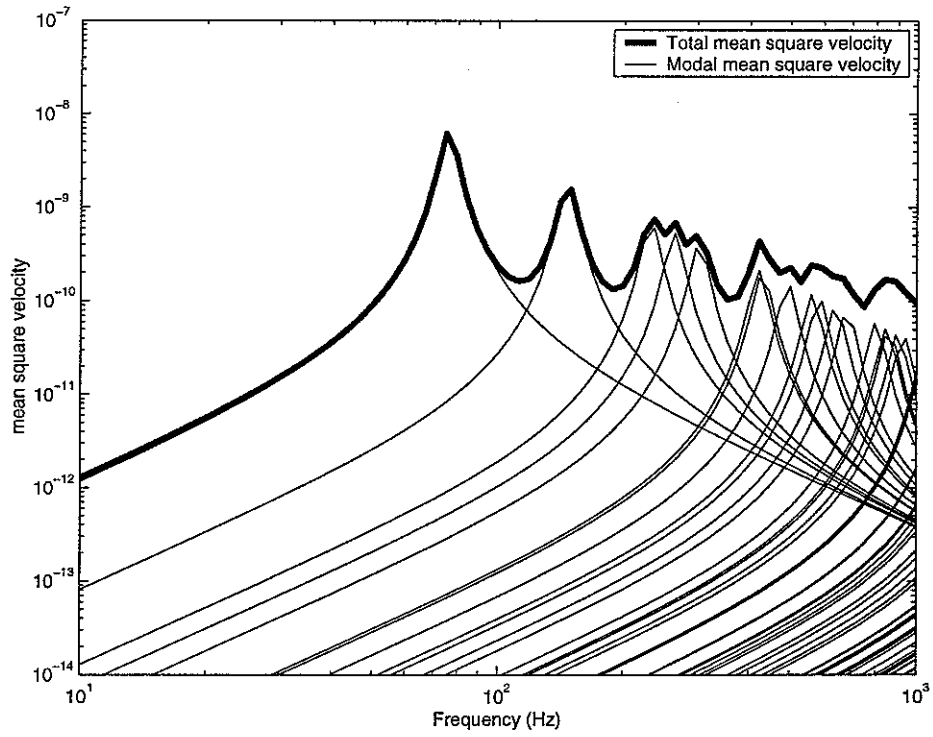

**Figure 4.5 Average mean square velocity of the extruded plate showing contributions from global modes. (2.016 × 3.0 × 0.07m aluminium extruded plate with strip thickness 0.003m and $\eta = 0.1$)**

The calculation results are presented in Figure 4.5, Figure 4.6 and Figure 4.7. It can be seen that the first mode at 76Hz is the only mode below the critical frequency. This anticipates that, for frequencies below the critical frequency, Leppington's formula might not give a good agreement with the results from the summation of all mode contributions because it is based on a high modal density. This disagreement is confirmed by the comparison of results, as shown in Figure 4.7. The comparison shows that Maidanik's formula has a good agreement at frequencies below the first global mode of the extruded plate. However, for both Leppington's and Maidanik's formula the limiting values around the critical frequency are less than unity because $f_c$ is low. The values calculated are 0.90 and 0.91 respectively (see section 3.4 for details). These have therefore not been applied in Figure 4.7.

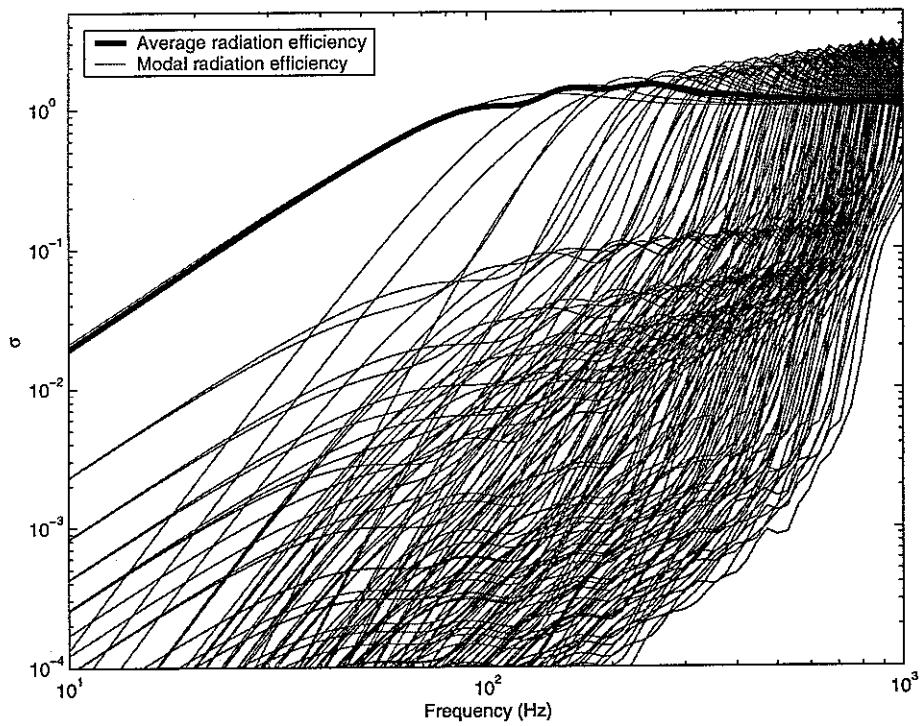


**Figure 4.6 Modal and average radiation efficiency of the global modes of the extruded plate.**

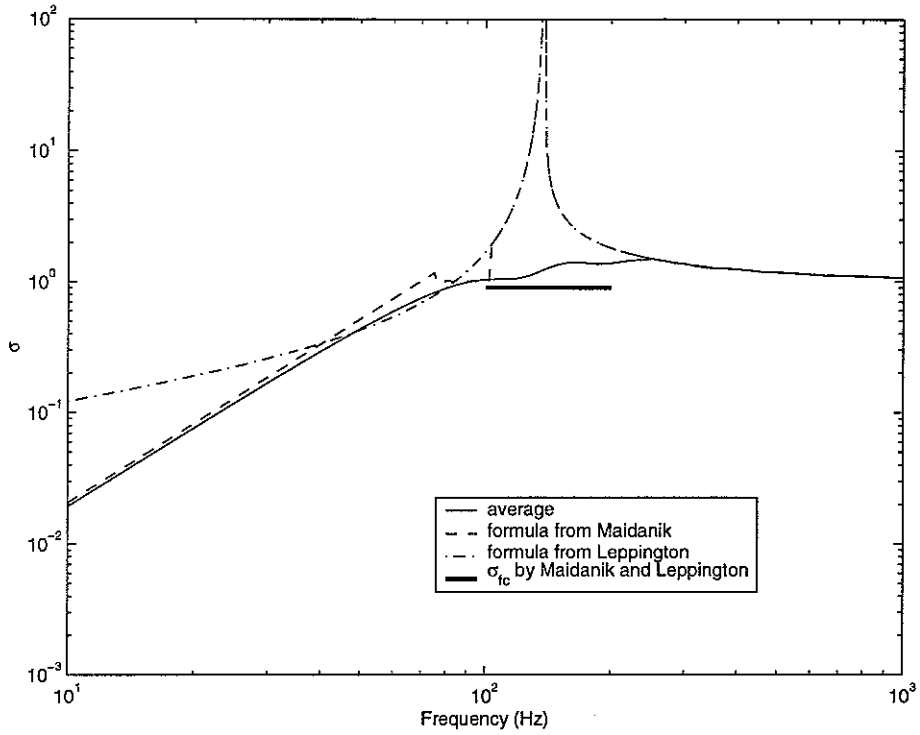


**Figure 4.7 Average radiation efficiency of the global modes of the extruded plate.**

## 4.2 RADIATION FROM LOCAL MODES

The radiation efficiency from local modes can be analysed by considering each strip independently. Each strip vibrates with a certain velocity amplitude in a baffled plane. The distribution of velocity over the strip is similar to that under the boundary conditions of simple supports. Then each strip can be treated by following the procedure carried out for the strips described in section 3.

However, the amplitude distribution of the velocity of the local modes over all strips due to a point force applied on the surface of the extruded plate is unknown at present. The simplest approximation is to assume that the vibration is localised to the strip excited directly by the point force due to the modal localization, provided that the dimensions of strips are different from each other, and thus only that strip radiates sound. This means that the term for local modes in equation (4.1) depends on a 'single' strip and should be weighted over the entire surface depending on the excitation point. The averaged radiated power from local modes for all possible excitation point can hence be given by

$$\overline{W}_{local} = \sum_i \frac{A_i}{A} \overline{W}_i \tag{4.8}$$

where $A$ is the area of the surface of the extruded plate, $i$ under the summation indicates the $i$th strip on the surface of the extruded plate, $A_i$ is the area of the $i$th strip, and $W_i$ is the averaged power radiated by the $i$th strip, which is given by

$$\overline{W}_i = \rho c A_i \sigma_i \overline{\langle u_i^2 \rangle} \tag{4.9}$$

where $\sigma_i$ and $\overline{\langle u_i^2 \rangle}$ are the radiation efficiency and spatially averaged mean square velocity corresponding to $i$th strip respectively.

For a system with many modes of vibration, the mean square velocity is approximately given by

$$\overline{\langle u_i^2 \rangle} = \frac{W_{in}}{\omega \eta \rho_s h A_i} \tag{4.10}$$

where $\overline{W_{in}} = \frac{1}{2}|P|^2 \overline{\mathrm{Re}(Y)}$ is the input power averaged over forcing positions on plate $i$. For an average over forcing locations $\overline{\mathrm{Re}(Y)}$ is similar on each strip. Thus the average square velocity on each strip is proportional to $1/A_i$. But the likelihood of a point force occurring on a given strip is proportional to $A_i$ (equation (4.8)).

The spatially averaged mean square velocity of the whole plate for excitation on plate $A_i$ is

$$\overline{\langle u_l^2 \rangle} = \frac{A_i}{A} \overline{\langle u_i^2 \rangle} = \frac{W_{in}}{\omega \eta \rho_s h A} \tag{4.11}$$

which is the same for excitation on any strip.

The radiated power for excitation on the $i$th strip can be rewritten as

$$W_i = \rho c A_i \sigma_i \overline{\langle u_i^2 \rangle} = \rho c \sigma_i \frac{W_{in}}{\omega \eta \rho_s h} = \rho c \sigma_i A \overline{\langle u_l^2 \rangle} \tag{4.12}$$

Hence equation (4.8) can be rewritten as

$$\overline{W}_{local} = \overline{\langle u_l^2 \rangle} \sum_i \rho c A_i \sigma_i \tag{4.13}$$

where $u_l$ is the spatially averaged velocity due to local modes.

## 4.3 OVERALL RADIATION FROM EXTRUDED PLATES

The averaged radiation efficiency of the extruded plate over all possible forcing points on one side can be now considered through equation (4.2). This gives

$$\sigma = \frac{\overline{W}_{global} + \overline{W}_{local}}{\rho c A \overline{\langle u^2 \rangle}} = \frac{\sigma_g \overline{\langle u_g^2 \rangle} + \overline{\langle u_l^2 \rangle} \sum_i \frac{A_i}{A} \sigma_i}{\overline{\langle u_g^2 \rangle} + \overline{\langle u_l^2 \rangle}} \tag{4.14}$$

where $u_g$ is the velocity due to global modes, $u_l$ is the velocity due to local modes.

Obviously, the calculation of equation (4.14) requires the knowledge of the spatially averaged mean square velocity for global modes and local modes, radiation efficiencies for global modes and for each strip. In the present report, the radiation efficiency for global modes and each strip have been modelled. However, the prediction of the velocities of global and local modes needs further work. One approach is to find the modal density of the extruded plate. For a structure, the mean square velocity can be given in terms of modal density by [16]

$$\overline{\langle u^2 \rangle} = \overline{P}^2 \frac{\pi n(\omega)}{2\eta m^2 \omega} \tag{4.15}$$

where $\overline{P}$ is the r.m.s value of the force applied, $n(\omega)$ is the modal density of the structure under consideration, $\eta$ is the damping loss factor and $m$ is the mass of the structure.

If the modal density of the global modes and local modes were found, the mean square responses of the two sets of modes can be estimated. Therefore, the calculation for the radiation efficiency of the extruded plate will be carried out once these modal densities of the extruded plate have been found. This is the subject of a further report.

# 5 CONCLUSIONS

The radiation efficiency of rectangular plates has been investigated. It has been demonstrated that the total radiation can be calculated without including the cross-mode contribution if, as is usual in SEA, an average over all possible forcing points is considered. The averaged radiation efficiency based on the modal summation approach shows the limitations of previous formulae by Maidanik [1] and Leppington [6] for a strip, a plate with a large aspect ratio. It has been shown that its radiation efficiency below the fundamental frequency is proportional to the square of the shortest edge rather than the area of the plate. For frequencies between the fundamental mode and second cut-on, the radiation from the strip can be considered to be equivalent to the radiation of two edge monopoles each of size $a \times \lambda_y/4$ where $\lambda_y$ is the wavelength along the length of the strip. The near-field radiation efficiency in this region appears to be proportional to

the damping loss factor. It is found that the dependence of the near-field radiation efficiency for the strip on the damping loss factor is approximately twice that for the rectangular plate.

Based on the results from the modal summation approach, it is found that the maximum average radiation efficiency increase proportionally with $(ka_1)^{1/4}$ for $ka_1 > 3$, not $(ka_1)^{1/2}$ as Leppington's and Maidanik's, where $k$ is the acoustical wavenumber and $a_1$ is the shorter edge of the plate. For $ka_1 < 3$, the radiation efficiency tends to the constant from 1.2 to 1.3 for different aspect ratio.

The radiation efficiency of extruded plates has been considered in terms of global modes and local modes. The characteristics of the radiation of the global modes are equivalent to that of a rectangular plate which has a low critical frequency. The radiation of the local modes is treated as strips. An approximation for the calculation of the radiation efficiency of extruded plates has been given. As the expressions for the modal density for global and local modes of the extruded plates are still under investigation, the final results will be presented in a subsequent report.

# REFERENCES


1. G. Maidanik 1962 *Journal of the Acoustical Society of America* **34**, 809-826. Response of ribbed panels to reverberant acoustic fields.
2. C. E. Wallace 1972 *Journal of the Acoustical Society of America* **51**, 946-952. Radiation resistance of a rectangular panel.
3. M. C. Gomperts 1974 *Acustica* **30**, 320-327. Radiation from rigid baffled rectangular plates with general boundary conditions.
4. M. C. Gomperts 1977 *Acustica* **37**, 93-102. Sound radiation from baffled, thin, rectangular plates.
5. M. Heckl, 1977 *Acustica* **37**, 155-166. Radiation from plane sound sources.
6. F. G. Leppington, E. G. Broadbent and K. H. Heron 1982 *Proceedings of the Royal Society London* A **382**, 245-271. The acoustic radiation efficiency of rectangular panels.
7. E. G. Williams 1983 *Journal of the Acoustical Society of America* **73**, 1520-1524. A series expansion of the acoustic power radiated from planar sources.
8. W. L. Li 2001 *Journal of Sound and Vibration* **245**(1), 1-16. An analytical solution for the self-and mutual radiation resistances of a rectangular plate.
9. I. L. Ver, and C. I. Holmer. 1971. *In* "Noise and Vibration Control" (L. L. Beranek, ed.), pp. 287-296. McGraw-Hill, New York.
10. S. Snyder and N. Tanaka 1995 *Journal of the Acoustical Society of America* **97**, 1702-1709. Calculating total acoustic power output using modal radiation efficiencies.
11. W. L. Li and H. J. Gibeling 1999 *Journal of Sound and Vibration* **229**, 1213-1233. Determination of the mutual radiation resistances of a rectangular plate and their impact on the radiated sound power.
12. W. L. Li and H. J. Gibeling 1999 *Journal of Sound and Vibration* **220**, 117-133. Acoustic radiation from a rectangular plate reinforced by finite springs at arbitrary locations.
13. G. Xie, D. J. Thompson and C. J. C. Jones 2002 *ISVR Technical Memorandum* **No: 882**. Investigation of the mode count of one-dimensional systems.
14. K. Sakagami, K. Michishita, M. Morimoto and Y. Kitamura 1998 *Applied Acoustics* **55**, 181-202. Sound radiation from a baffled elastic plate strip of infinite length with various concentrated excitation forces.
15. Lord Rayleigh 1896 *The Theory of Sound* 2nd ed. (reprinted by Dover, New York, 1945).

16. L. Cremer, M. Heckl and E. E. Ungar 1988 *Structure-borne Sound.* Berlin: Springer-Verlag; second edition.
17. M. J. Crocker and A. J. Price 1969 *Journal of Sound and Vibration* **9**(3), 469-486. Sound transmission using statistical energy analysis.
18. F. J. Fahy, 1985 *Sound and Structural Vibration*: *Radiation, Transmission and Response.* London: Academic Press.
19. S. P. Timoshenko, S. Woinowsky-Krieger, 1959 *Theory of Plate and Shells,* 2nd Edition, Ch. 11, McGraw-Hill.
20. M. Heckl, 1960 *Acustica* **10**, 109-115. Untersuchungen an orthotropen platten.